Distribution of the Auxiliary $GABA_B$ Receptor Subunits KCTD8, 12, 12b, and 16 in the Mouse Brain

Michaela Metz,[1] Martin Gassmann,[1] Bernd Fakler,[2,3] Nicole Schaeren-Wiemers,[4]* and Bernhard Bettler[1]*

[1]Department of Biomedicine, Institute of Physiology, University of Basel, 4056 Basel, Switzerland
[2]Institute of Physiology II, University of Freiburg, 79108 Freiburg, Germany
[3]Center for Biological Signaling Studies (bioss), 79104 Freiburg, Germany
[4]Department of Biomedicine, Neurobiology Laboratory, University Hospital Basel, 4031 Basel, Switzerland

ABSTRACT

$GABA_B$ receptors are the G-protein-coupled receptors for γ-aminobutyric acid (GABA). KCTD8, 12, 12b, and 16 were recently identified as auxiliary $GABA_B$ receptor subunits and distinctly influence biophysical and pharmacological properties of the receptor response. Here we examined the expression patterns of the KCTDs in the mouse brain. Using in situ hybridization analysis, we found that most neurons express KCTD transcripts, supporting biochemical data showing that most $GABA_B$ receptors in the brain incorporate KCTD proteins. In the adult brain, KCTD12 and 16 have a widespread and KCTD8 and 12b a restricted expression pattern. Individual neurons can coexpress multiple KCTDs, as shown for granule cells and CA1/CA3 pyramidal cells in the hippocampus that coexpress KCTD12 and 16. In contrast, granule, Purkinje, and Golgi cells in the cerebellum selectively express one KCTD at a time. The expression levels of individual KCTD transcripts vary during postnatal brain development. Immunohistochemistry reveals that individual KCTD proteins can exhibit distinct axonal or dendritic localizations in neuronal populations. KCTDs are also detectable in nonneuronal tissues not expected to express $GABA_B$ receptors, suggesting that the role of KCTD proteins extends beyond $GABA_B$ receptors. In summary, our findings support that most brain $GABA_B$ receptors associate with KCTD proteins, but that the repertoire and abundance of KCTDs varies during development, among brain areas, neuronal populations, and at subcellular sites. We propose that the distinct spatial and temporal KCTD distribution patterns underlie functional differences in native $GABA_B$ responses. J. Comp. Neurol. 519:1435–1454, 2011.

INDEXING TERMS: γ-aminobutyric acid; GABA-B; GABAB; GPCR; KCTD12; KCTD16

$GABA_B$ receptors are expressed throughout the brain and considered attractive drug targets because they are implicated in the etiology of neurological and psychiatric disorders (Bettler et al., 2004). They influence synaptic transmission by regulating the activity of voltage-activated Ca^{2+} (Cav), inward-rectifier K^+ (Kir) channels, and by decreasing local cAMP levels. The kinetic and pharmacological properties of $GABA_B$ responses vary among neurons and between effectors, which suggests the existence of a variety of molecularly distinct receptor subtypes (Bonanno and Raiteri, 1993; Cunningham and Enna, 1996; Deisz et al., 1997; Cruz et al., 2004). However, for a long time the heterogeneity of native $GABA_B$ responses contrasted with the molecular identification of only two receptors with equivalent properties in transfected cells (Ulrich and Bettler, 2007). The two receptors are based on the subunit isoforms $GABA_{B1a}$ and $GABA_{B1b}$ that combine with a $GABA_{B2}$ subunit to form heteromeric $GABA_{B(1a,2)}$ and $GABA_{B(1b,2)}$ receptors. Possibly resolving the puzzling discrepancy between recombinant and neuronal studies, we recently identified the four K^+ channel tetramerization domain (KCTD)-containing proteins KCTD8, 12, 12b, and 16 as auxiliary $GABA_B$ receptor subunits (Schwenk et al., 2010). While little information on KCTD proteins is available, a single-nucleotide polymorphism

Additional Supporting Information may be found in the online version of this article.

Grant sponsor: Swiss Science Foundation; Grant number: 3100A0-117816; Grant sponsor: Fridericus Stiftung and the European Community's 7th Framework Programme; Grant number: FP7/2007-2013 under Grant Agreement 201714 (to B.B.); Grant sponsor: Deutsche Forschungsgemeinschaft; Grant number: SFB 746/TP16; SFB 780/A3; EXC294 (to B.F.).

*CORRESPONDENCE TO: Bernhard Bettler, Department of Biomedicine, Institute of Physiology, Pharmazentrum, University of Basel, 4056 Basel, Switzerland. E-mail: bernhard.bettler@unibas.ch or Nicole Schaeren-Wiemers, Department of Biomedicine, Neurobiology, Zentrum für Lehre und Forschung, University Hospital Basel, 4031 Basel, Switzerland. E-mail: nicole.schaeren-wiemers@unibas.ch

Received October 28, 2010; Revised December 21, 2010; Accepted February 1, 2011
DOI 10.1002/cne.22610
Published online February 25, 2011 in Wiley Online Library (wileyonlinelibrary.com)

in the vicinity of the KCTD12 gene is associated with bipolar I disorder (Lee et al., 2010). Coexpression of KCTD proteins with the core receptors $GABA_{B(1a,2)}$ and $GABA_{B(1b,2)}$ in cultured cells replicates kinetic and pharmacological properties of native $GABA_B$ responses. KCTD proteins assemble as a tetramer with the $GABA_{B2}$ subunit. It is currently unclear whether distinct KCTD proteins can simultaneously bind to $GABA_{B2}$ and whether this fine-tunes the receptor response. Clearly, understanding the native role of the KCTD proteins relies on a comprehensive analysis of their expression patterns at the cellular and subcellular level. Moreover, since the core receptor subunits $GABA_{B1a}$ and $GABA_{B1b}$ are differentially expressed during postnatal development (Malitschek et al., 1998; Fritschy et al., 1999, 2004; Lopez-Bendito et al., 2002, 2004; Lujan and Shigemoto, 2006), it is important to study the developmental KCTD expression pattern. In this study we used northern blots, in situ hybridization, and immunohistochemistry to provide a first account of the spatial and temporal expression patterns of KCTD8, 12, 12b, and 16 in the brain. We discuss the implications of our findings for $GABA_B$ receptor physiology.

MATERIALS AND METHODS

Animals and brain sections

Brain sections of adult and postnatal day 5 (P5) BALB/c mice were used for in situ hybridization and immunohistochemistry. Mice were anesthetized with isoflurane (Baxter, Deerfield, IL), decapitated, the brains removed, embedded in O.C.T. compound (Sakura Finetek, Zoeterwoude, Netherlands), and snap-frozen in liquid nitrogen. Heads of P5 mice were embedded as a whole. Ten-μm sections were cut with a Microm HM 560 cryomicrotome (Microm, Walldorf, Germany). Animal experiments were conducted in accordance with Swiss guidelines and approved by the veterinary office of Basel-Stadt.

Generation of KCTD cDNA probes

Mouse cDNA inserts for generating random primed cDNA probes and riboprobes were amplified from non-coding regions with lowest homology and subcloned into pGEM-T easy (Promega, Madison, WI). Two independent probes for KCTD8 and 16 and four probes for KCTD12b were generated to control for specificity: KCTD8 (AY615967, bp 1–216, 1–1088), KCTD12 (NM_177715, bp 2709–4998), KCTD12b (NM_17542, bp 1–298, 1137–1637, 1879–2325, 3233–3708), and KCTD16 (XM_909931, bp 2423–4735, 4736–6465).

Northern blots

Northern blots containing 20 μg total RNA of various adult mouse tissues were purchased from Zyagen Laboratories (San Diego, CA). Total RNA from cerebral cortex and cerebellum was isolated from adult mouse brain, separated on a formaldehyde agarose gel, and transferred to a nylon membrane as described previously (Lai and Lemke, 1991). Hybridization was done with PerfectHyb Plus buffer (Sigma, St. Louis, MO) at 68°C with ^{32}P-labeled random primed cDNA probes.

In situ hybridization

Antisense and sense (control) digoxigenin-labeled riboprobes were generated using T3 and T7 RNA polymerase (Roche Diagnostics, Mannheim, Germany), respectively. Riboprobes against neuron-specific enolase (NSE) were generated as described before (Schaeren-Wiemers et al., 1997). Digoxigenin-labeled riboprobes were alkaline hydrolyzed to an average length of 200–400 bases and used for hybridization as described previously (Schaeren-Wiemers and Gerfin-Moser, 1993). The alkaline phosphatase color reaction was stopped at different timepoints between 1 and 4 days to grade transcript expression levels. In situ hybridization with NSE cRNA probes on adjacent sections was consistently used to establish cellular identities.

Semiquantitative analysis of transcript levels

KCTD transcript expression levels were graded relative to the NSE hybridization signal (Schaeren-Wiemers et al., 1997). KCTD transcript expression levels in cells were classified as follows: very strong (++++), strong (+++), moderate (++), weak (+), and no detectable signal (−). A punctuated staining reflecting expression in isolated cells was indicated with (o) (Tables 2, 3).

Immunohistochemistry

Cryostat sections of adult mouse brains were fixed for 1 hour in 10% phosphate-buffered saline (PBS) buffered formalin solution, washed 3 times in PBS (pH 7.4), and incubated overnight at room temperature in 70% ethanol. Unspecific binding sites were blocked by incubation with 2.5% normal goat serum, 0.1% fish skin gelatin, 0.15% Triton X-100 in PBS for 45 minutes at room temperature. Incubation with primary antibodies (anti-KCTD8, anti-KCTD12, anti-KCTD16 [Schwenk et al., 2010]; anti-neurofilament 200 (Sigma); anti-NeuN [Chemicon, Temecula, CA]; anti-$GABA_{B2}$ [Chemicon]) was done overnight at 4°C in blocking solution. Primary antibodies were detected with fluorophore-conjugated secondary antibodies (Alexa Fluor 488/647, Invitrogen, Carlsbad, CA) and sections mounted with Fluorosafe (Calbiochem, San Diego, CA). Alternatively, primary antibodies were detected using the Vector Elite ABC-Kit (Vector Laboratories, Burlingame, CA). Endogenous peroxidase activity was blocked by incubation with 0.6% H_2O_2 / 80% methanol in H_2O for 20 minutes at room temperature. The peroxidase substrate AEC (3-amino-9-ethylcarbazole, 0.027% w/v; H_2O_2 0.03% v/v) in 0.1 M

TABLE 1.
Primary Antibodies Used

Antibody	Immunogen	Manufacturer	Dilution used
KCTD8	Synthetic peptide, aa 374-391 of mouse KCTD8	Pineda (Berlin, Germany), rabbit polyclonal	1:1,000
KCTD12	Synthetic peptide, aa 145-167 of mouse KCTD12	Pineda (Berlin, Germany), rabbit polyclonal	1:1,000
KCTD16	Synthetic peptide, aa 7-23 of mouse KCTD16	Pineda (Berlin, Germany), rabbit polyclonal	1:1,000
$GABA_{B2}$	Synthetic peptide from the C-terminus of $GABA_{B2}$, aa 921-940 of rat or 922-941 of human	Chemicon (Temecula, CA), guinea pig polyclonal, AB5394	1:1,000
NeuN	Purified cell nuclei from mouse brain	Chemicon (Temecula, CA), mouse monoclonal, MAB377	1:500
Neurofilament 200	Neurofilaments purified from pig spinal cord	Sigma (St. Louis, MO), mouse monoclonal, N5389, clone NE14	1:1,000

sodium acetate buffer pH 5.2 was used for the 10-minute color reaction at room temperature in the dark. Duplicate sections were weakly counterstained with Mayer's Haemalaun (Merck, Darmstadt, Germany) for 1 minute. Sections were embedded in Kaiser's glycerin gelatin (Merck).

Antibody characterization

Please see Table 1 for a list of all primary antibodies used. The KCDT8 antibody recognized a single band of 52 kD molecular weight on western blots of wildtype but not of KCTD8 knockout brain homogenates (Supplementary Fig. 1), and produces an immunostaining pattern consistent with the KCTD8 in situ hybridization analysis. The KCDT12 antibody recognized a single band of 36 kD molecular weight on western blots of wildtype but not of KCTD12 knockout brain homogenates (Supplementary Fig. 1). In addition, KCTD12 immunoreactivity was not detected on cryosections of KCTD12 knockout brains. The KCDT16 antibody recognized a single band of 47 kD molecular weight on western blots of wildtype but not of KCTD16 knockout brain homogenates (Supplementary Fig. 1). In addition, KCTD16 immunoreactivity was not detected on cryosections of KCTD16 knockout brains. The $GABA_{B2}$ antiserum recognized a single band of ≈110 kD molecular weight on western blots of wildtype but not of $GABA_{B2}$ knockout brain homogenates (Gassmann et al., 2004). The pattern of $GABA_{B2}$ immunoreactivity with this antiserum in the mouse brain is identical to the pattern described previously (Fritschy et al., 2004). The NeuN antibody stained only nuclei, and in a neuronal pattern consistent with previous findings in the mouse brain (Mullen et al., 1992). The Neurofilament 200 antibody specifically recognizes the neurofilaments of molecular weight 200 kD and does not crossreact with other intermediate filament proteins (manufacturer's technical information). It stained axonal projections from the medial habenula along the fasciculus retroflexus (Fig. 9)

Image acquisition and processing

Images were captured with a Leica DMRE microscope (Leica, Wetzlar, Germany) equipped with a high-resolution digital camera, using ColorView IIIu for brightfield, F-View for fluorescence microscopy, and AnalySIS software (SIS, Münster, Germany). Images were adjusted for brightness/contrast and assembled using Adobe PhotoShop CS4 (v. 11.0) / Adobe Illustrator CS4 (v. 14.0.0; Adobe Systems, San Jose, CA). Brain structures are labeled according to Franklin and Paxinos (2001).

RESULTS

KCTD transcripts are predominantly but not exclusively expressed in the nervous system

Northern blot analysis of various adult mouse tissues revealed that KCTD8, 12, and 16 transcripts are predominantly expressed in the brain (Fig. 1A). For KCTD8 a single 3.5 kb transcript was detected in the brain but not in other tissues analyzed. For KCTD12 a 6 kb transcript was detected at high levels in the brain and at low levels in the intestine, colon, kidney, heart, testis, and bone marrow. For KCDT16 a 9 kb transcript was detected in the brain and spinal cord. In addition, a larger KCTD16 transcript of ≈15 kb was detected in a number of nonneuronal tissues, in particular in the intestine, suggesting that this subtype is differentially spliced. KCTD12b transcripts were below the detection level in the brain and spinal cord. However, a 5-kb KCTD12b transcript was observed in the kidney, heart, ovary, and adipose tissue at varying expression levels. Northern blot analysis of adult cortex and cerebellum revealed a differential expression pattern of KCTD8, KCDT12, and KCTD16 (Fig. 1B). While KCTD12 is highly expressed in both areas, KCTD8 shows a higher expression in the cerebellum, whereas KCTD16 is more prominent in the cerebral cortex, suggesting that the KCTD subtypes are differentially expressed within the brain.

General features of KCTD expression in the brain

A comprehensive in situ hybridization analysis was performed in adult and P5 mouse brain. Results of the semiquantitative analysis of KCTD8, 12, and 16 transcript expression levels of the analyzed brain areas are provided

TABLE 2.

Distribution of KCTD Transcripts in the Adult Mouse Brain

	KCTD8	KCTD12	KCTD16
Olfactory bulb			
Olfactory nerve layer	–	++++	–
Glomerular layer	++	+	+
External plexiform layer	–	+	–
Mitral layer	++	++/o	++
Granular layer	+	+	+
Anterior olfactory nucleus	–	++	++
Olfactory tubercle	–	+	++
Islands of Calleja	–	–	++
Piriform area, layer II	–	++	+++
Basal ganglia			
Caudate putamen	+	+	+++
Globus pallidus	–	+	–
Nucleus accumbens	+	++	+
Ventral pallidum	–	+	+
Claustrum	–	+	+++
Endopiriform nucleus	–	–	+++
Septum			
Medial septum	–	+++	–
Lateral septum, caudal	–	++	+
Lateral septum, rostral	–	++++	+++
Cortex			
Frontal			
Layer I-III	+	+ / O	+++
Layer V	+	+	–
Layer VI	–	+ / O	++
Layer VIb, isocortex	–	+ / O	++
Parietal			
Layer MI	+	+ /O	++++
Layer III	+	+ /O	++++
Layer IV	–	+ /O	+++
Layer V	+	+ /O	+
Layer VI	–	+ /O	+++
Layer VIb, isocortex	–	+ /O	+++
Amygdala			
Basolateral nuclei			
Anterior	–	+	++
Posterior	–	+++	+++
Basomedial nuclei	–	+	+
Central nucleus	+	+++	+
Medial nucleus			
Anteroventral	–	–	+
Posterodorsal	+	++	++
Lateral nucleus	–	+	+++
Cortical amygdalar area	–	++	++++
Piriform amygdalar area, layer II	–	++	++++
Bed nucleus stria terminalis	–	+++	+
Hippocampal formation			
Pyramidal layer CA1	+	+++	++++
Pyramidal layer CA2	–	++++	+++
Pyramidal layer CA3	–	+++	+++
Dentate gyrus, granular layer	–	++++	++++
Hilar cells/polymorphic layer	+	+++	+++
Subiculum	++	+	++
Entorhinal cortex, layer II	–	+++	+++
Induseum griseum	–	+++	+++
Taenia tecta	–	++	++
Thalamus			
Anterior group			
Anterodorsal	–	+	–
Laterodorsal	–	–	+++
Anteroventral	–	–	+++
Ventral medial	–	++	+++
Ventral posteromedial	–	++	+++
Ventral posterolateral	–	+	+++
Subparafascicular nucleus	–	+	+++
Posterior group	–	+	+++
Rhomboid nucleus	–	++	+++
Reunions nucleus	–	+	++
Reticular thalamic nucleus	–	–	++
Geniculate group			
Medial geniculate nuclei	–	+	++
Lateral geniculate nuclei, dorsal		–	+++
Lateral geniculate nuclei, ventral	–	–	+
Epithalamus			
Medial habenula	++++	+	–
Lateral habenula	+	+	+
Hypothalamus			
Medial preoptic area	–	+++	–
Lateral preoptic area	–	+++	–
Nucleus of the diagonal band	–	++	–
Magnocellular preoptic nucleus	–	+++	+
Dorsomedial hypothalamic	+	+	++
Lateral hypothalamic area	–	++	+
Posterior hypothalamic nucleus	–	++	+
Mammillary bodies	–	–	++++
Zona incerta	+	+	+++
Cerebellum			
Molecular layer	–	–	–
Granular layer			
Granule cells	++	–	–
Golgi cells	–	–	+++
Purkinje cells	–	++++	–
Deep cerebellar nuclei	+	+	++
Brainstem			
Midbrain			
Olivary pretectal nucleus	–	–	++
Anterior pretectal nucleus	–	+	++
Substantia nigra, Pars compacta	–	+	+
Substantia nigra, Pars reticulata	–	+	+
Ventral tegmental area	–	+	+
Interpeduncular nucleus	+	+	++
Mesencephalic reticular nucleus	–	–	–
Superior colliculi			
Superficial gray layer	+	+	++
Optical layer	+	+	+++
Periaqueductal grey	–	+	+
Inferior colliculus	+	+	+++
Raphe nucleus dorsalis/central	+	+	++
Parabigeminal nucleus	+	+++	–
Nucleus of the optic tract	+	+	+
Pons			
Locus coeruleus	–	+	+
Pontine reticular nuclei	+	++	+
Parabrachial nucleus	+	+	+
Nucleus of the lateral lemniscus	–	+	++
Superior olivary complex	–	+	+
Nucleus of the trapezoid body	–	++	–
Medulla oblongata			
Spinal nucleus of trigeminal	++	++	+
Facial motor nucleus	+	+	+
Vestibular nuclei	+	+	+
Nucleus prepositus	+	+	+
Dorsal cochlear nucleus	++	+++	+

	KCTD8	KCTD12	KCTD16		KCTD8	KCTD12	KCTD16
Medial group				Ventral cochlear nucleus	++	+	+
Mediodorsal	+	++	+++	Dorsal motor nucleus of the vagus nerve	+	+	+
Paraventricular	–	+	–	Hypoglossal nucleus	++	++	+
Ventral group				Inferior olivary complex	–	++	–
Ventral anterior-lateral complex	–	+	++	External cuneate nucleus	+	++	–

Intensities of in situ hybridization signal: ++++, very strong; +++, strong; ++, moderate; +, weak; o, expression in isolated cells; -, no detectable signal.

in Table 2 (adult) and Table 3 (P5). The combined data from horizontal (Schwenk et al., 2010) and coronal (Fig. 2) sections reveal distinct but partly overlapping KCTD expression patterns. In general, KCTD12 and 16 transcripts are expressed throughout the brain (Fig. 2C,D). KCTD12 shows highest expression levels in the septum, the hippocampal formation, and the cerebellum. High KCTD16 transcript levels were primarily observed in the cortex, the hippocampal formation, and the thalamus. These brain areas are known for high $GABA_B$ receptor expression levels (Bischoff et al., 1999; Margeta-Mitrovic et al., 1999). KCTD8 transcripts are restricted to a few brain areas, such as the medial habenula (MH, Fig. 2B), certain brainstem nuclei, and the granule cell layer of the cerebellum (Table 2). KCTD12b transcripts are only detectable in the medial habenula (see Fig. 9), consistent with KCTD12b expression being below detection level in whole-brain RNA extract (Fig. 1A).

Select neuronal populations express distinct subsets of KCTD transcripts. For example, pyramidal and dentate granule cells of the hippocampus express high levels of KCTD12 and 16 transcripts, while neurons in the medial habenula express KCTD8, 12, and 12b transcripts. In contrast, different cell types in the cerebellum mostly express one KCTD transcript at the time. Here we provide a detailed description of the transcript expression pattern of each KCTD protein in the mouse brain. To investigate the subcellular localization of the KCTD proteins we performed immunofluorescence microscopy and immunohistochemistry in select brain areas.

Olfactory system

Highest KCTD transcript expression levels are observed in the olfactory nerve layer containing the axons of olfactory receptor neurons entering the olfactory bulb (ONL, Fig. 3). KCTD12 transcripts are expressed throughout the olfactory nerve layer in cells lacking NSE expression (open arrow, Fig. 3C). Most likely, these cells represent olfactory ensheathing cells, which constitute the major glial component of the olfactory nerve (Franklin and Barnett, 2000). The presence of KCTD12 protein in the olfactory nerve layer was confirmed by immunofluorescence microscopy (ONL, Fig. 3C, inset).

KCTD transcripts are also found in neurons of the main olfactory bulb. KCTD8, 12, and 16 transcripts are observed in some periglomerular neurons in the glomerular layer (arrows, Fig. 3B–D), as well as in subsets of neurons in the mitral cell layer (arrowheads, Fig. 3B–D). Neurons in both layers express high levels of $GABA_B$ receptors (Panzanelli et al., 2004).

Expression of KCTD12 transcripts in the olfactory ensheathing cells is already detectable at P5 in the olfactory nerve layer (open arrow, Fig. 3E) and in the lamina propria of the olfactory mucosa (LP, open arrow, Fig. 3G). At this developmental stage olfactory receptor neurons in the olfactory epithelium express KCTD16 transcripts (OE, open arrowheads; Fig. 3H). This suggests that mainly $GABA_B$ receptors assembled with KCTD16 are the $GABA_B$ receptors present in olfactory receptor neurons (Panzanelli et al., 2004). In the adult, high levels of KCTD12 and 16 transcripts are also found in the target areas of projection fibers of the main olfactory bulb, including the anterior olfactory nucleus, olfactory tubercle, taenia tecta, piriform, and entorhinal cortices (Table 2).

Basal ganglia

Several KCTD transcripts are expressed in the dorsal part of the basal ganglia (Table 2). The caudate putamen reveals high levels of KCTD16 (CP, Fig. 2D), while KCTD8 and 12 are much less abundant (Fig. 2B,C). In the globus pallidus only KCTD12 could be detected (Table 2). In the ventral part of the basal ganglia the nucleus accumbens expresses moderate levels of KCTD12 and low levels of KCTD8 and 16, while the ventral pallidum expresses low levels of KCTD12 and 16 (Table 2). Remarkably, very high levels of KCTD16 are observed in the claustrum (CLA, Fig. 4D), where other KCTD transcripts are mostly absent (Fig. 4B,C). The claustrum is a telencephalic subcortical structure that projects to and receives input from a number of cortical areas (Crick and Koch, 2005). Notably, the claustral complex is involved in propagation of epileptiform activity from the amygdala and the severity of seizures is related to GABAergic activity (Sheerin et al., 2004; Zhang et al., 2001).

TABLE 3.

Distribution of KCTD Transcripts at Postnatal Day 5

	KCTD8	KCTD12	KCTD16		KCTD8	KCTD12	KCTD16
Olfactory bulb	–	++	–	Subparafascicular nucleus	–	+	+++
Olfactory nerve layer (ensheating glia)	–	++++	–	Posterior group	–	+	+++
Anterior olfactory nucleus	–	++	+++	**Geniculate group**			
Granule cell layer	–	++	–	Medial geniculate nuclei	–	+++	++
Basal ganglia				Lateral geniculate nuclei	–	++++	++
Caudate putamen	++	+++	+++	**Hypothalamus**			
Globus pallidus	–	+++	–	Mammillary bodies	–	–	++++
Claustrum	–	–	+++	**Cerebellum**			
Septum	+	+++	++	Purkinje cell layer	–	+++	+
Cortex				Deep cerebellar nuclei	–	+	+++
1	–	+++	+++	External granule cell layer	+++	+	–
II-III	–	–	+	Internal granule cell layer	–	+++	+
IV	–	+	+++	**Midbrain**/ Pans/ **Medulla**			
V	–	+	–	Superior colliculus	+	++	+
VI	–	+++	+	Inferior colliculus	+	++++	++
VIb	–	–	–	Parabigeminal nucleus	–	+++	–
Amygdala				Dorsal cochlear nucleus	++	+++	+
Lateral	++	++/O	+++	Ventral cochlear nucleus	++	+	+
Basolateral	–	+	+++	Nucleus of the lateral lemniscus	–	+	++
Central	–	++	–	Superior olivary complex	+++	+	++
Hippocampal formation				Spinal nucleus of trigeminal	++	++	+
Pyramidal layer CA1	+	+ / O	+++	**Peripheral tissues**			
Pyramidal layer CA2	–	+++	+++	Retina			
Pyramidal layer CA3	–	+++	+	Ganglion cell layer	–	++++	+++
Dentate gyms, granular layer	–	+++	+	Inner nuclear layer	++++	–	++
Hilar cells/polymorphic layer	–	+	+	Olfactory mucosa			
Subiculum	++	++	+	Olfactory epithelium	–	–	++++
Thalamus				Lamina propria (ensheating glia)	–	++++	–
Anterior group of the dorsal thalamus				Cochlea, Spiral ganglion	++	++++	+
Anterodorsal	–	+	–	Trigeminal ganglion	++	+/O	++++
Laterodorsal	–	–	+++	Inferior glossopharyngal ganglion	–	++++	++
Anteroventral	–	–	+++	Whisker	–	+++	–
Medial group				Dental pulp	–	+++	–
Mediodorsal nucleus	+	+	+++	Bone marrow	–	++++	–
Ventral group							
Ventral posteromedial	–	+	+++				
Ventral posterolateral	–	+	+++				

Intensities of in situ hybridization signal: ++++, very strong; +++, strong; ++, moderate; +, weak; o, expression in isolated cells; -, no detectable signal.

Septum

The lateral septum, a major recipient of hippocampal output, shows high expression levels of KCTD12 and 16 transcripts (Fig. 4G,H), which correlates with high expression levels of $GABA_{B1}$ transcripts and $GABA_B$ antagonist binding sites in this area (Bischoff et al., 1999). Highest levels of KCTD12 transcripts are observed in the neurons of the rostral part of the lateral septum (LSr, Fig. 4G), which project to the hypothalamic medial zone nuclei, in particular the anterior hypothalamic nucleus, which is known for prominent expression of $GABA_B$ receptors (Margeta-Mitrovic et al., 1999). The medial septal nucleus, containing mainly GABAergic and cholinergic neurons projecting to the hippocampus, selectively expresses KCTD12 (Table 2). No KCTD8 transcripts are detected in the septum (Fig. 4F, Table 2). Expression patterns at P5 resemble those observed in adult mice (Table 3). In summary, the data imply that mainly KCTD12 and 16 participate in septal $GABA_B$ receptor complexes.

Cerebral cortex

We examined the frontal and parietal cortex for KCTD transcripts. The frontal cortex is an agranular isocortical area, representative of the primary motor cortex. In contrast, the parietal cortex has a clearly visible inner granular layer (layer IV) and is representative of the somatosensory cortex (Zilles, 1990). In both cortices KCTD transcripts exhibit very distinct expression patterns (Table 2). KCTD16 is uniformly expressed throughout the cortical layers with the exception of layer V, where it is only expressed by a small number of neurons (Fig. 5D). KCTD12 is weakly expressed throughout layers II, III, and layer V (Fig. 5C). In addition, strong expression of KCTD12 is observed in a number of large neurons, most

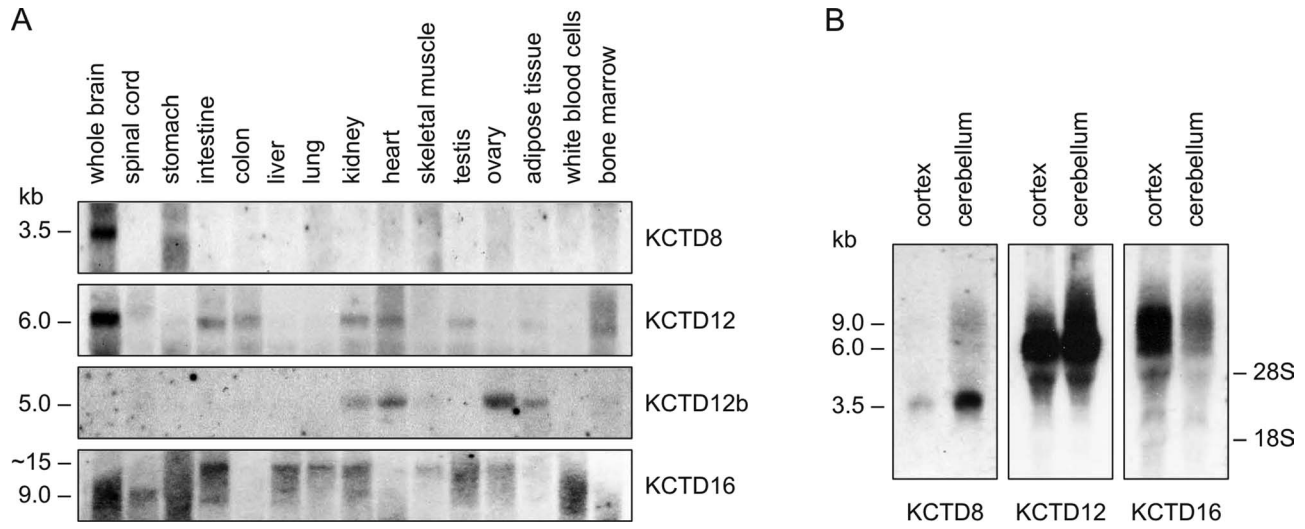

Figure 1. Expression analysis of KCTD transcripts in mouse tissues. Northern blot analysis of total RNA from various adult tissues (**A**) and adult cerebral cortex and cerebellum (**B**). The molecular weights of prominent KCTD transcripts are indicated on the left. In (B) the size of the 18S and 28S ribosomal RNA bands are indicated on the right.

likely interneurons, scattered throughout all layers (arrowheads, insets; Fig. 5C). KCTD12 expression in these neurons was confirmed by immunohistochemistry, which reveals high amounts of KCTD12 protein in the cell bodies and neuropil (Fig. 5J–L). On the basis of their size and their stellate-like morphology, these cells may be large basket cell interneurons. KCTD8 is detectable at very low expression levels in layers II, III, and layer V (Fig. 5B). The KCTD expression patterns in the P5 cerebral cortex differ markedly from those in the adult. At P5, KCTD8 is not detectable in the entire cortex (Fig. 5G). KCTD12 is strongly expressed in a large number of cells in the inner layers of the cortex, predominantly layer VI, and in dispersed cells in the outer layers (Fig. 5H). Conversely, KCTD16 is predominantly expressed in the outer cortical layers (Fig. 5I). Notably, no $GABA_{B1b}$ expression in the cortex is detectable at P5 (Bischoff et al., 1999; Fritschy et al., 2004), suggesting that at P5 KCTD12 and 16 mostly combine with the $GABA_{B(1a,2)}$ core receptor.

Amygdala

The amygdala is part of the limbic system and implicated in psychiatric conditions (LeDoux, 2000). $GABA_B$ receptors inhibit glutamatergic inputs to the lateral amygdala and control synaptic plasticity processes in the amygdala (Shaban et al., 2006). The amygdala is composed of several nuclei (Swanson and Petrovich, 1998; LeDoux, 2007), with distinct KCTD transcript distribution patterns (Fig. 6). KCTD16 is highly abundant in principal cells of the lateral amygdala nucleus (LA, Fig. 6D,H) and the basolateral nucleus (BLA, Fig. 6D,H). KCTD12 is primarily detected in a subpopulation of principal cells in the BLA (open arrowheads, Fig. 6C,G), in the central amygdala (CEA, Fig. 6C), and in the posterodorsal part of the medial nucleus (Table 2). Sparsely scattered cells expressing KCD12 in the basolateral nucleus most likely represent local interneurons. The central amygdala is one of the few amygdala nuclei that, in addition to KCTD12 and 16 transcripts, also express low levels of KCTD8 transcripts (Fig. 6B–D). Very high levels of KCTD16 and moderate levels of KCTD12 transcripts are expressed in cortical amygdala areas (Table 2). Finally, high and low levels of KCTD12 and 16 transcripts, respectively, are detected in the bed nucleus of the stria terminalis, which belongs to the extended amygdala (Table 2).

Hippocampal formation

Because of the well-described localization and functions of $GABA_B$ receptors in the hippocampal formation (Kulik et al., 2003; Lopez-Bendito et al., 2004; Vigot et al., 2006; Guetg et al., 2009), the KCTD transcript distribution in this structure is of particular interest. High levels of KCTD12 and 16 transcripts are present in the granular layer (g) of the dentate gyrus and in the pyramidal cell layer (p) of the CA regions (Fig. 7B,C). Within the CA regions KCTD12 expression levels are highest in CA2 and CA3 (Fig. 7B), whereas KCTD16 expression levels are highest in CA1 (Fig. 7C). KCTD12 and 16 are also highly expressed in a subset of putative dentate pyramidal basket cells located at the border between the granule cell layer and the hilus of the dentate gyrus (arrowheads, Fig. 7B,C insets). In addition, high KCTD12 and 16 expression levels are observed in a variety of nonpyramidal cells throughout the hippocampus (arrows, Fig. 7B,C), most

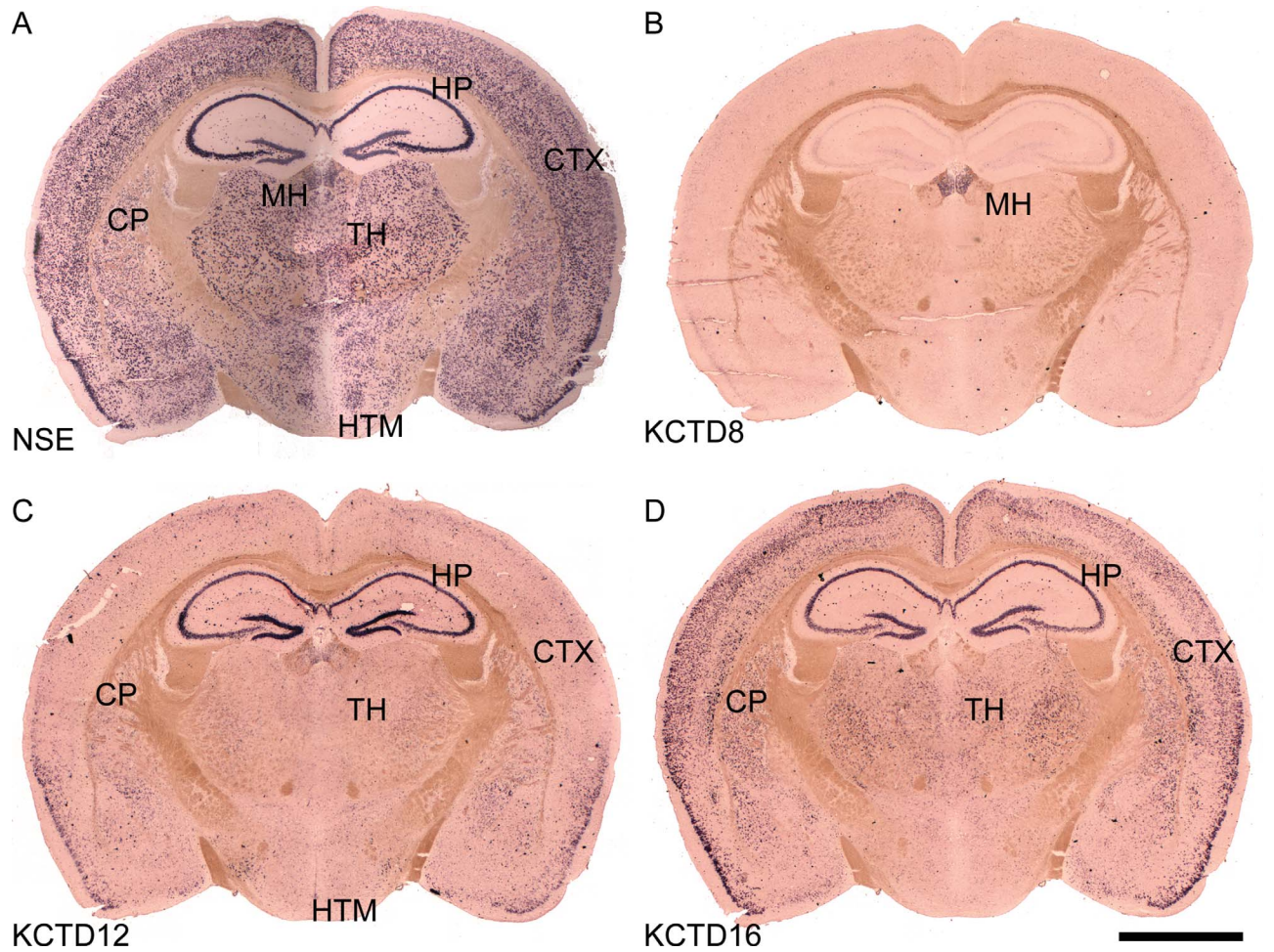

Figure 2. Overview of KCTD transcript distribution in adult mouse brain. Brightfield images showing the localization of neuron-specific enolase (NSE, **A**) and KCTD8, 12, and 16 transcripts (**B–D**) in one representative coronal brain section. Caudate putamen (CP), cerebral cortex (CTX), hippocampus (HP), hypothalamus (HTM), medial habenula (MH), and thalamus (TH). Scale bar = 2 mm.

likely GABAergic local circuit interneurons (Franklin and Paxinos, 1997). Many of these KCTD expressing interneurons are located in the stratum radiatum (r) and stratum lacunosum-moleculare (lm) and may therefore correspond to interneuronal populations that preferentially innervate the distal dendritic regions targeted by excitatory afferent pathways (Sloviter et al., 1999). Neurons in the subiculum contain low levels of KCTD12 and high levels of KCTD8 and KCTD16 (Table 2). The subiculum sustains afferent and efferent connections to the entorhinal cortex. High KCTD12 and 16 transcript levels are predominant in layer II of the entorhinal cortex (Table 2), which contains mainly stellate cells that are the principal source of fibers for the perforant path projection to the dentate gyrus and the CA3. At P5, KCTD12 is strongly expressed in hippocampal CA2 and CA3 regions, in the dentate gyrus, and in many cells scattered throughout the stratum oriens, stratum radiatum, and the stratum lacunosum-moleculare (Fig. 7E), similar to the adult. KCTD16, however, is generally weakly expressed in the developing hippocampus and barely detectable in the dentate gyrus (Fig. 7F). KCTD8 expression could only be detected in the subiculum (S, Fig. 7D), similar to the adult (Table 3). Immunofluorescence microscopy in the dentate gyrus of adult mice revealed a differential localization of the KCTD proteins (Fig. 7G–J). KCTD12 immunoreactivity is prominent in the outer molecular layer (m, asterisk, Fig. 7G), most likely reflecting KCTD12 protein in distal dendrites of granule cells. KCTD16 immunoreactivity, however, is observed at the soma and neuropil of granule cells (Fig. 7I, inset). In agreement with prominent $GABA_{B2}$ expression throughout the molecular layer of the dentate gyrus (Kulik et al., 2003; Fritschy et al., 2004; Lopez-Bendito et al., 2004), we observed a colocalization of $GABA_{B2}$ and KCTD12 in the outer molecular layer (asterisk, Fig. 7H) and of $GABA_{B2}$ and KCTD16 in a narrow band along the granule cell layer (asterisk, Fig. 7J). In addition, a colocalization of KCTD16 and $GABA_{B2}$ was also

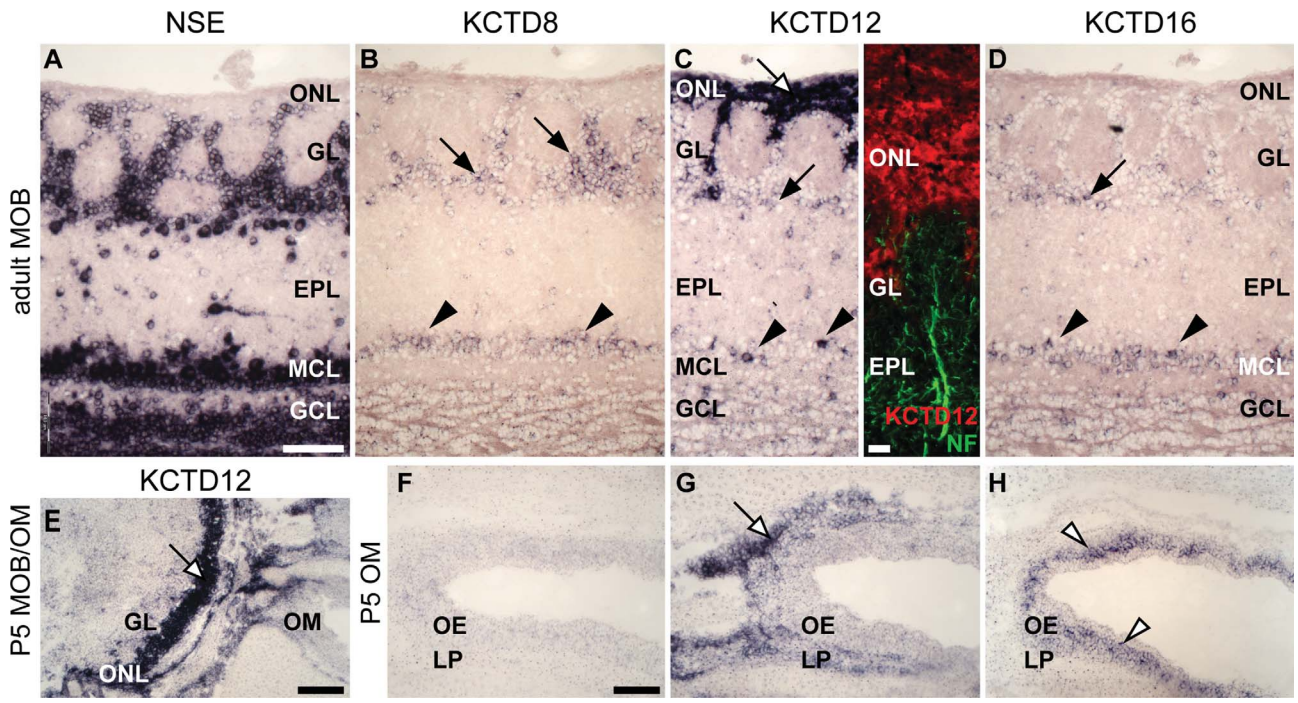

Figure 3. KCTD expression in the mouse olfactory system. The expression pattern of NSE transcripts is shown for comparison (**A**). KCTD8 (**B**), 12 (**C**), and 16 (**D**) transcripts are expressed in a small subset of neurons in the glomerular (GL) and mitral cell layer (MCL). Nonneuronal olfactory ensheathing cells (OEC) in the olfactory nerve layer (ONL) show very high KCTD12 transcript levels (open arrow, C,**E**). KCTD12 protein expression in the OECs is demonstrated by immunofluorescence microscopy of the adult olfactory bulb (C, inset; KCTD12 in red; neurofilament [NF] in green). At P5 KCTD8 is not detectable in the olfactory mucosa (**F**), whereas KCTD12 is expressed in OECs (open arrow, **G**) and KCTD16 in the olfactory epithelium (open arrowheads, **H**). EPL, external plexiform layer; GCL, granule cell layer of the olfactory bulb, GL, glomerular layer; LP, lamina propria; MCL, mitral cell layer; MOB, main olfactory bulb; OE, olfactory epithelium; OM, olfactory mucosa; ONL, olfactory nerve layer. A magenta-green copy of this figure is available as Supplementary Fig. 2. Scales bar = 200 μm, inset 50 μm.

observed in the neuropil of the dentate hilus (h, Fig. 7J inset), a region containing the axons of the granule cells. Strong KCTD12 immunoreactivity was also observed in putative dentate pyramidal basket cells located at the granule cell–hilus border (arrowheads, Fig. 7G,H), in agreement with the in situ hybridization data (arrowheads, Fig. 7B inset).

Thalamus

The thalamus is important for the processing of somatosensory, visual, and auditory input to the cortex. The thalamus is one of the areas in the brain showing highest $GABA_B$ receptor levels (Kaupmann et al., 1998; Princivalle et al., 2000; Lopez-Bendito et al., 2003). KCTD16 is expressed in almost all nuclei of the thalamus, generally at moderate to high levels (Fig. 8D,H, Table 2). KCTD12 expression is moderate in few nuclei but generally low (Fig. 8C,G). KCTD8 expression is not detectable in most thalamic nuclei (Fig. 8B,F). Remarkably, individual nuclei in the anterior thalamus express only one KCTD subtype at the time. KCTD12 is weakly expressed in the anterodorsal nucleus (AD, Fig. 8C), while KCTD16 is expressed in the laterodorsal (LD) and the anteroventral (AV) nucleus (Fig. 8D). The mediodorsal nucleus (MD) of the medial group is one of the few thalamic nuclei coexpressing KCTD8, 12, and 16 (Table 2). Apart from the mediodorsal nucleus, KCTD12 is expressed moderately in the ventral medial (VM) and the ventral posteromedial (VPM) nucleus (Fig. 8C,G). Finally, moderate to high levels of KCTD16 transcripts are observed in the posterior group of the thalamus (PO, Fig. 8H), in the geniculate nucleus (Table 2, Fig. 8H), and the subparafascicular nucleus (Table 2). In summary, our data suggest that in the adult thalamus $GABA_B$ receptors predominantly incorporate KCTD16. At P5, the KCTD expression pattern in the thalamus is reminiscent of the adult expression pattern (Table 3). KCTD16 is expressed at high levels throughout the thalamus, while KCTD12 is only expressed at low levels in the anterodorsal nucleus of the anterior group and in the medial and ventral group of the dorsal thalamus. At P5, KCTD12 is highly expressed in the geniculate nuclei, in contrast to the adult.

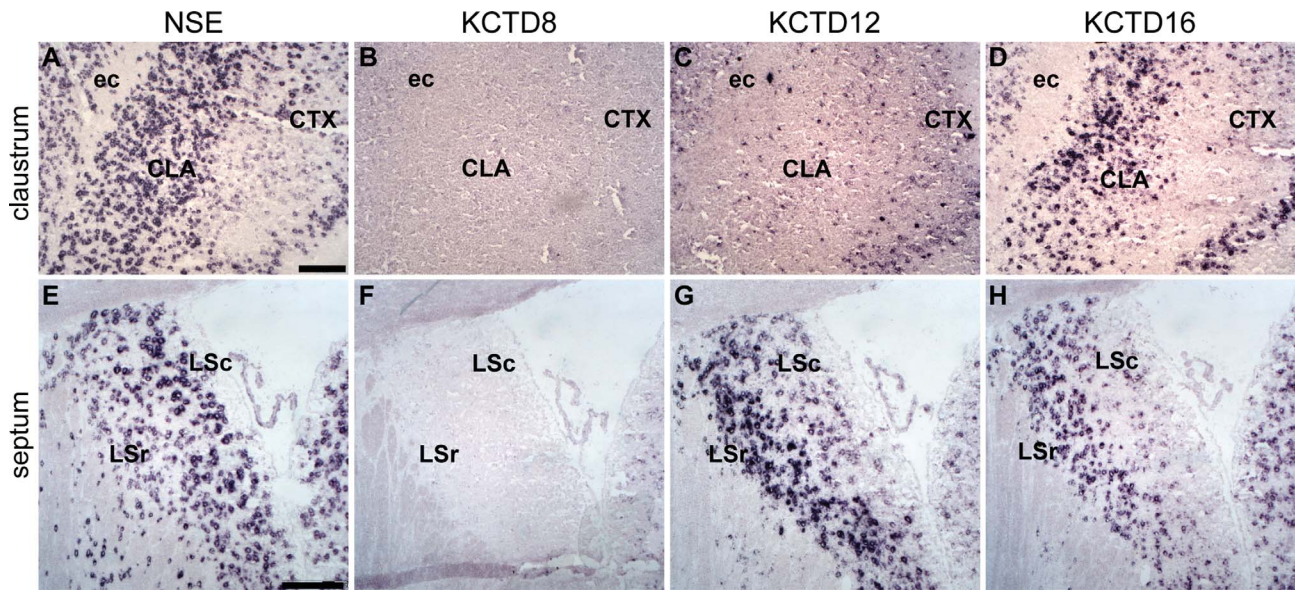

Figure 4. KCTD transcript distribution in claustrum and septum of adult mouse brain. NSE is shown for comparison (**A**,**E**). In the claustrum KCTD8 (**B**) is not detectable. KCTD12 (**C**) is expressed in a small subset of neurons. KCTD16 is expressed at very high levels (**D**). In the septum KCTD8 is not detectable (**F**). KCTD12 is expressed at very high (**G**) and KCTD16 at high (**H**) levels in the rostral part of the lateral septum. CLA, claustrum; CTX, cortex; ec, external capsule; LSc, lateral septum: caudal part; LSr, lateral septum: rostral part. Scale bars = 200 μm.

Epithalamus

The medial habenula is a cholinergic nucleus projecting through the fasciculus retroflexus to the interpeduncular nucleus (habenulo-interpeduncular tract). The function of the habenulo-interpeduncular connection is poorly understood. Evidence from rodents supports that this connection controls avoidance, reward, and feeding behaviors (Sutherland, 1982). The medial habenula is among the brain areas expressing highest levels of $GABA_B$ receptors (Bischoff et al., 1999; Fritschy et al., 2004). We found that this brain area expresses high levels of KCTD8 and 12 transcripts (MH, Fig. 9A,B). Of particular interest, the medial habenula is the only brain region where KCTD12b transcripts are detectable (MH, Fig. 9C). Moderate levels of KCTD16 transcripts are found in the lateral habenula (LH), in contrast to the complete absence of KCTD16 in the medial habenula (Fig. 9D). Immunofluorescence microscopy reveals abundant KCTD8 expression in neurons of the medial habenula and their axonal projections along the fasciculus retroflexus (FR, arrow, Fig. 9E,F). In agreement with the previously described intense immunolabeling for $GABA_B$ receptors (Fritschy et al., 2004), KCTD8 and $GABA_{B2}$ prominently colocalize in the fasciculus retroflexus (FR, arrow, Fig. 9G).

Hypothalamus

KCTD12 transcripts are more abundant in the hypothalamus than in the thalamus (Fig. 2C). The highest levels of KCTD12 transcripts are observed in the anterior part of the hypothalamus, including the medial and the lateral preoptic area, the nucleus of the diagonal band, and the magnocellular preoptic nucleus (Table 2). Moderate levels of KCTD12 transcripts are also detected in the lateral hypothalamic area and the posterior hypothalamic nucleus. The anterior nuclei receive input from the lateral septum and control body temperature. Notably, mice with a genetic lack of $GABA_B$ receptors exhibit hypothermia (Kaupmann et al., 2003). This is likely caused by the loss of $GABA_B$ receptors in the hypothalamus, which are important for the control of body temperature (Pierau et al., 1997). KCTD12 transcripts are less abundant in other areas of the hypothalamus, where KCTD16 transcripts are more highly expressed (Table 2). In particular, very high levels of KCTD16 transcripts are detected in the mammillary bodies and high levels in the zona incerta. KCTD16 expression in the mammillary bodies is already detectable at P5 (Table 3). KCTD8 expression in adult mice is only seen in a few hypothalamic nuclei (Table 2).

Brainstem (midbrain/pons/medulla)

$GABA_B$ receptors are expressed in several regions of the brainstem (Durkin et al., 1999; Margeta-Mitrovic et al., 1999). Generally low to moderate expression levels of KCTD transcripts are observed in brainstem. KCTD8 and 16 transcripts are most prominent in certain nuclei of the medulla oblongata and the midbrain, respectively

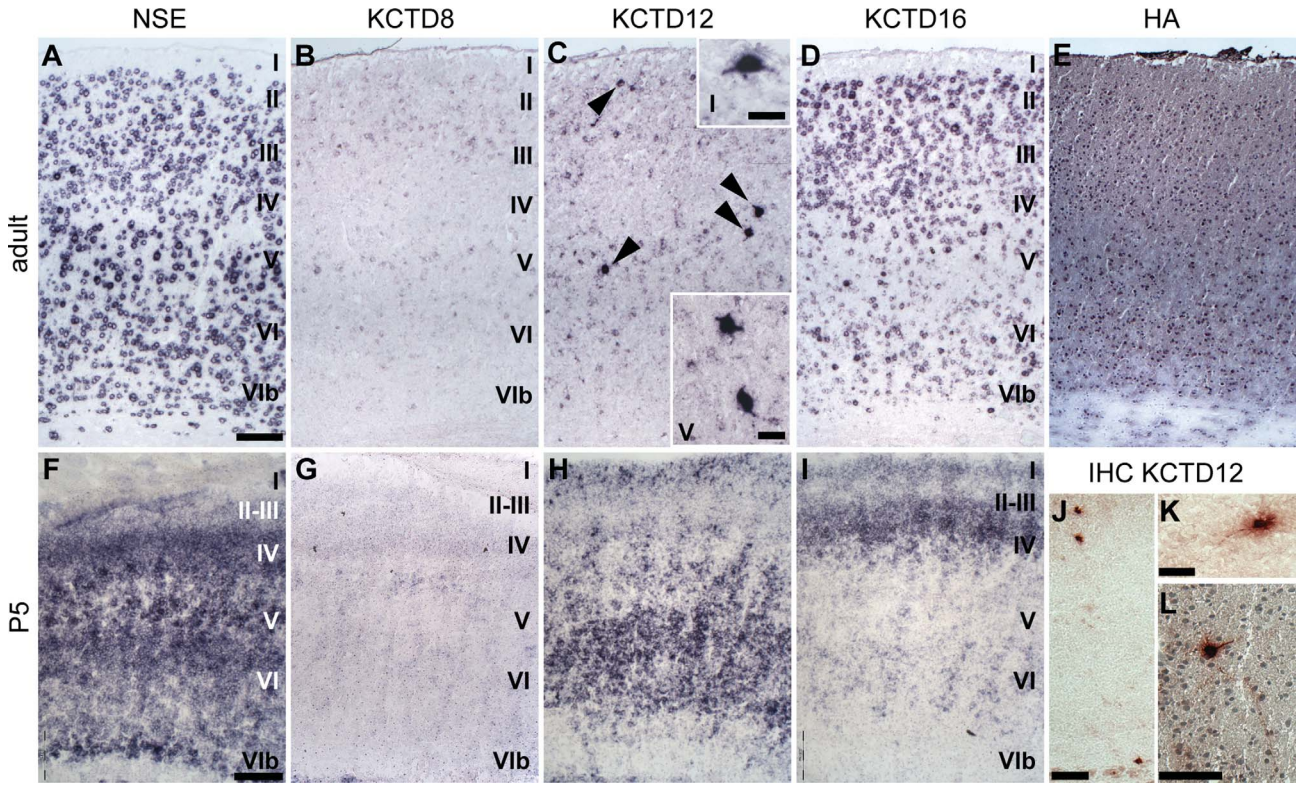

Figure 5. KCTD expression in layers of the mouse primary sensory cortex. NSE expression is shown for comparison (**A,F**). In the adult KCTD8 transcripts are weakly expressed in layer II, III and V (**B**). KCTD12 transcripts are highly enriched in a number of large neurons scattered throughout all cortical layers (arrowheads and insets layer I and V, **C**); a comparable expression pattern is observed with immunoperoxidase staining for KCTD12 protein (**J–L**). KCTD16 transcripts are highly abundant in all cortical layers, except layer V (**D**). Haemalaun (HA) staining is shown on an adjacent section (**E**). At P5, KCTD8 is not detectable (**G**). KCTD12 and 16 transcripts levels are high in the inner (**H**) and in the outer cortical layers (**I**), respectively. IHC, immunohistochemistry. Scale bars = 200 μm; 100 μm in L; 50 μm in C (insets, K).

(Table 2). KCTD16 is moderately expressed in the anterior pretectal nucleus, as well as in the olivary pretectal nucleus and in the superior colliculus (Table 2), which are target areas of retinal inputs. KCTD8 and 12 expression is low and high, respectively, in the parabigeminal nucleus (PBG, Fig. 10B,C), a subcortical visual center rich in $GABA_B$ receptors (Margeta-Mitrovic et al., 1999).

KCTD12 and 16 are present in the main brain areas and nuclei involved in auditory processing (Table 2). These include the inferior colliculus expressing high levels of KCTD16, the nucleus of the lateral lemniscus consisting of GABA- and glycinergic neurons expressing KCTD12 and 16, the superior olivary complex, and the nucleus of the trapezoid body expressing KCTD12 (Table 2). Additionally, we found that the dorsal cochlea nucleus in which auditory nerve fibers from the cochlea form their first synapses display high levels of KCTD8 and 12, and low levels of KCTD16 transcripts (DCN, Fig. 10F–H). The superior and inferior colliculi abundantly express $GABA_B$ receptors (Margeta-Mitrovic et al., 1999). Interestingly, both colliculi express high levels of KCTD12 transcripts at P5 but low levels in the adult. This contrasts with KCTD16 transcripts that are expressed at low levels at P5 but at very high levels in the adult (Tables 2, 3). KCTD12 is expressed at moderate levels in other brainstem nuclei, including the pontine reticular nuclei, the inferior olivary complex, and the external cuneate nucleus (Table 2).

Cerebellum

In the cerebellum KCTD transcripts show very distinct expression patterns (Fig. 11). KCTD8 transcripts are observed in the granule cell layer (GCL, Fig. 11B,F). KCTD12 shows very high transcript expression levels in Purkinje cells (arrows, Fig. 11C,G), which display the highest density of $GABA_B$ receptors in the cerebellum (Bischoff et al., 1999). Purkinje cells exhibit alternating stretches of labeled and nonlabeled cells (arrows, Fig. 11M) reminiscent of the Zebrin II zonation pattern (Brochu et al., 1990), which is more prominent in the anterior than in the posterior cerebellum. Immunohistochemistry and immunofluorescence microscopy with anti-KCTD12 antibodies confirm that the zebrin-like pattern is preserved in Purkinje cell dendrites of the molecular layer (ML, Fig. 11N–P). Strikingly, the striped

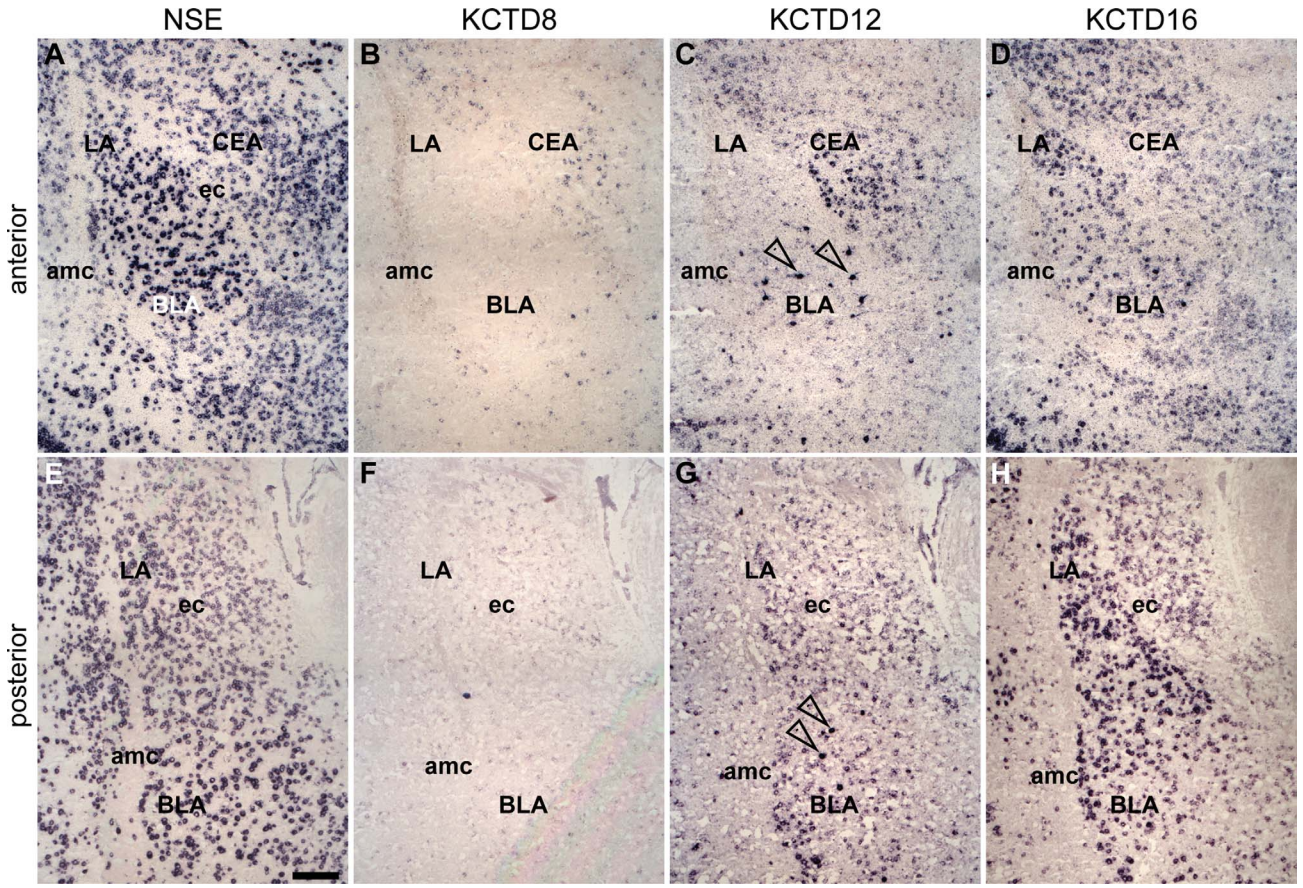

Figure 6. KCTD transcript distribution in the anterior and posterior nuclei of the adult mouse amygdala. NSE expression is shown for comparison (**A**,**E**). The central amygdala nucleus expresses KCTD8 (**B**), KCTD12 (**C**) and KCTD16 (**D**) transcripts. KCTD8 is not detectable in other amygdala nuclei (B,**F**). A population of cells in the basolateral amygdala strongly expresses KCTD12 transcripts (open arrowheads, C,**G**). KCTD16 is predominant in the lateral amygdala (D,**H**). amc, amygdala capsule; BLA, basolateral amygdala; CEA, central amygdala; ec, external capsule; LA, lateral amygdala. Scale bar = 200 μm.

pattern of KCTD12 immunoreactivity matches the pattern of $GABA_{B2}$ immunoreactivity in the molecular layer (Fig. 11Q), supporting that KCTD12 is part of $GABA_B$ receptors in Purkinje cell dendrites. The zebrin-like expression pattern for the $GABA_B$ receptor core subunits in the cerebellum was noted previously (Margeta-Mitrovic et al., 1999; Fritschy et al., 1999; Lujan and Shigemoto, 2006). KCTD16 mRNA is observed exclusively in large scattered cells in the cerebellar granular layer; putatively GABAergic Golgi cells (arrowheads, Fig. 11D,H). Finally, the deep cerebellar nuclei contain low levels of KCTD8, 12, and 16 (Table 2).

The cerebellum is one of the brain areas maturing during late embryonic and early postnatal development. From P7 onwards intense $GABA_{B1}$ immunoreactivity was reported in Purkinje cells, and moderate staining in the internal granular layer and migrating granule cells (Lujan and Shigemoto, 2006). At P5, KCTD12 is specifically expressed in differentiating Purkinje cells (open arrow, Fig. 11K) and in the internal granular layer (igl, Fig. 11K). At P5 the zebrin-like expression is not yet evident, as described for the $GABA_B$ receptor core subunits (Lujan and Shigemoto, 2006). At P5 KCTD8 is expressed in the external granular layer (egl, Fig. 11J), while KCTD16 transcripts are predominantly expressed in the deep cerebellar nuclei (Table 3).

Sensory systems

$GABA_B$ receptors are expressed in primary sensory neurons, the spinal cord, and the relay nuclei of several sensory pathways (Durkin et al., 1999). We analyzed KCTD expression levels at P5 and observed high KCTD expression levels in sensory systems.

Visual system

KCTD8, 12, and 16 transcripts are present in a subset of neurons of the retina (Fig. 12A–C) expressing $GABA_B$ receptors (Koulen et al., 1998). Our analysis detected KCTD12 mainly in retinal ganglion cells

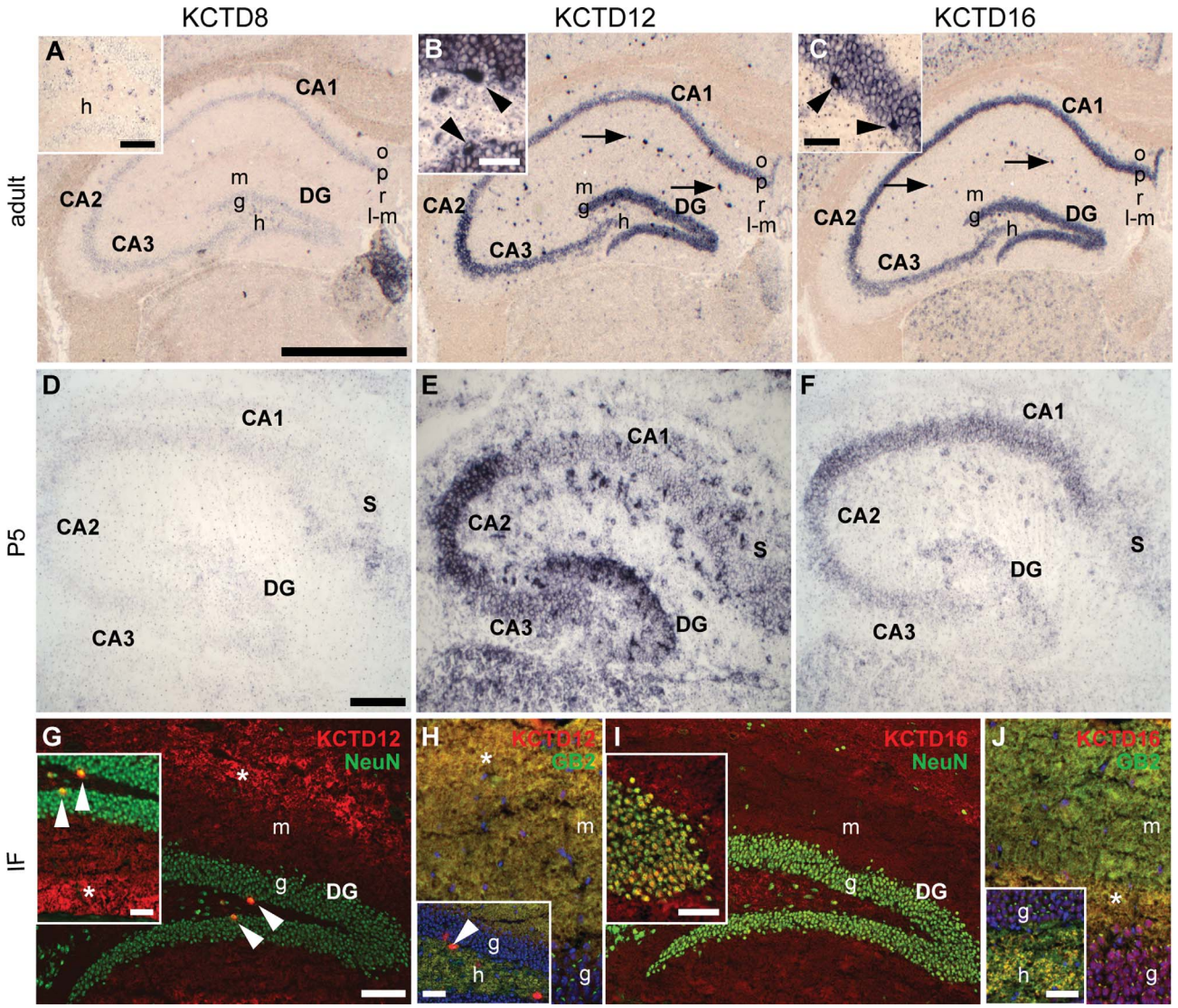

Figure 7. KCTD expression in the mouse hippocampus. In the adult, low levels of KCTD8 transcripts are expressed in hilar cells of the dentate gyrus (**A**, inset). KCTD12 and 16 transcripts exhibit strong expression in the pyramidal cell layer of the CA regions and the granular layer of the dentate gyrus (**B,C**). Both transcripts are also detected in nonpyramidal neurons (arrows) and a subset of interneurons in the dentate gyrus (arrowheads, B,C, insets). At P5, KCTD8 transcripts are present in the subiculum (**D**). Highest KCTD12 transcript levels are observed in pyramidal cells of the CA2 region and the dentate gyrus (**E**). Highest KCTD16 expression levels are observed in the CA1 region (**F**). Immunofluorescence microscopy in the dentate gyrus (**G–J**) reveals a differential protein localization for KCTD12 and 16 (in red). KCTD12 immunoreactivity is present in the outer molecular layer (G, asterisk) and in a subset of putative dentate pyramidal basket cells located at the border between the granule cell layer and the hilus of the dentate gyrus (arrowheads, G). In the outer molecular layer colocalization of KCTD12 and GABA$_{B2}$ is observed (H, asterisk), most likely reflecting GABA$_B$ receptor complexes in distal dendrites of granule cells. In contrast, GABA$_{B2}$ protein was not detectable in the KCTD12 expressing cells at the granule cell layer-hilus border (arrowhead, H, inset). KCTD16 is present in the soma and neuropil of granule cells (I). Colocalization of KCTD16 and GABA$_{B2}$ is observed in a narrow band along the granule cell layer (J, asterisk) and in the hilus (J, inset). CA1, CA2, CA3, fields of hippocampus; DG, dentate gyrus; S, subiculum; o, stratum oriens; p, stratum pyramidale; r, stratum radiatum; l-m, stratum lacunosum-moleculare; m, stratum moleculare; g, stratum granulosum; h, hilus; IF, immunofluorescence. A magenta-green copy of this figure is available as Supplementary Fig. 3. Scale bars = 1,000 μm in A–C; 50 μm in insets A–C,H–J; 200 μm in D–F; 100 μm in G–J.

(arrowheads, Fig. 12B), whereas KCTD8 is present in cells of the inner nuclear layer containing amacrine and bipolar cells (INL, Fig. 12A). KCTD16 expression, however, can be detected both in ganglion cells (arrowheads, Fig. 12C) and cells of in the inner nuclear layer (INL, Fig. 12C). As described above, KCTDs exhibit prominent expression in other brain areas that belong to the visual system (Table 2).

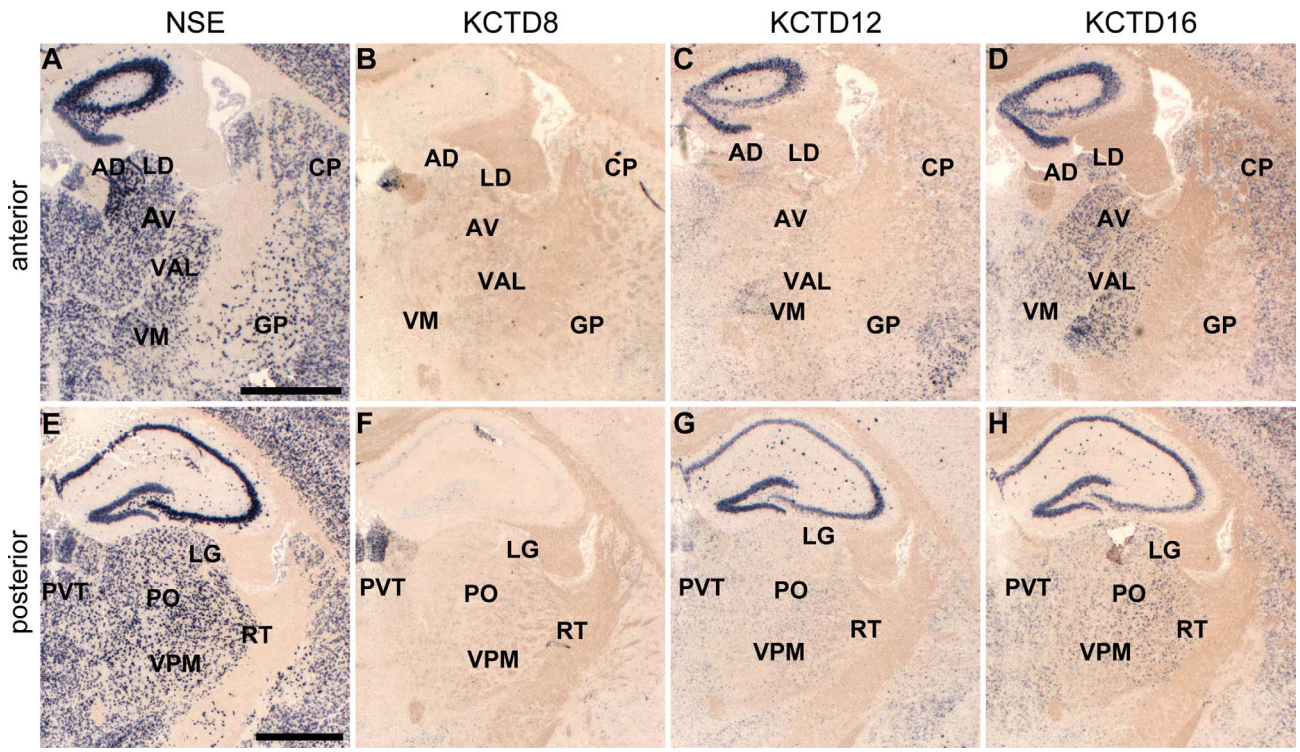

Figure 8. KCTD transcript distribution in the anterior and posterior thalamic nuclei of the adult mouse. NSE expression is shown for comparison (**A,E**). KCTD8 transcript expression is not observed in the anterior and posterior thalamus (**B,F**). KCTD12 transcripts are only found in some thalamic nuclei at low to moderate levels (**C,G**). KCTD16 shows high expression levels throughout the thalamus (**D,H**) with the exception of the anterodorsal nucleus of the thalamus (AD). AD, anterodorsal nucleus; AV, anteroventral nucleus; CP, caudate putamen; GP, globus pallidus; LD, laterodorsal nucleus; LG, lateral geniculate nucleus; MD, mediodorsal nucleus; PVT, paraventricular nucleus; PO, posterior group; RT, reticular thalamic nucleus; VAL, ventral anterior-lateral complex; VM, ventral medial nucleus; VPM, ventral posteromedial nucleus. Scale bars = 1,000 μm.

Auditory system

KCTD12 was first cloned from a human fetal cochlea library, which suggested that KCTD12 plays a role in the auditory system (Resendes et al., 2004). Consistent with this earlier report, we found KCTD12 to be highly expressed in the cochlea (Fig. 12E). Particularly, we found KCTD8, 12, and 16 expressed in spiral ganglia neurons (SG, Fig. 12D–F), which express functional $GABA_B$ receptors (Lin et al., 2000). Ganglion neurons receive GABAergic innervations from the lateral olivocochlear efferent system, originating from neurons located around the lateral superior olivary nucleus. $GABA_B$ receptors are present only in type I and type II ganglion cells, their dendrites within the cochlea, and their afferent terminals contacting inner and outer hair cells (Maison et al., 2009). Apart from the cochlea, KCTD12 and KCTD16 are present in many brain areas that are significantly involved in auditory processing (Table 2).

Sensory motor system

We observed KCTD8, 12, and 16 transcripts in structures of the whisker sensory motor system. KCTD8 and 16 are strongly expressed in the ganglion neurons of the trigeminal nerve (5Gn, Fig. 12G,I). In line with KCTD expression, $GABA_B$ receptors are present in ganglion neurons (Margeta-Mitrovic et al., 1999). A modulatory role for $GABA_B$ receptors was proposed in the processing of information at nociceptive primary afferents, which are the terminals of glutamatergic dorsal root and trigeminal ganglion cells (Reis and Duarte, 2006). Selectively, KCTD12 is expressed in whisker follicles (arrows, Fig. 12J). As described previously, KCTD12 and 16 are expressed in the ventral posterior medial and the posterior nuclei of the thalamus, which are part of the topographic somatosensory projection to the barrel field of the somatosensory cortex (Table 2). High levels of KCTD12 are also found in hair follicles (arrowheads, Fig. 12K). Finally, a striking observation was the unique and very high expression of KCTD12 in the odontoblast layer of the dental pulp of P5 mice (open arrows, Fig. 12L). It was reported that the odontoblast layer exhibits GABA staining (Todd et al., 1997).

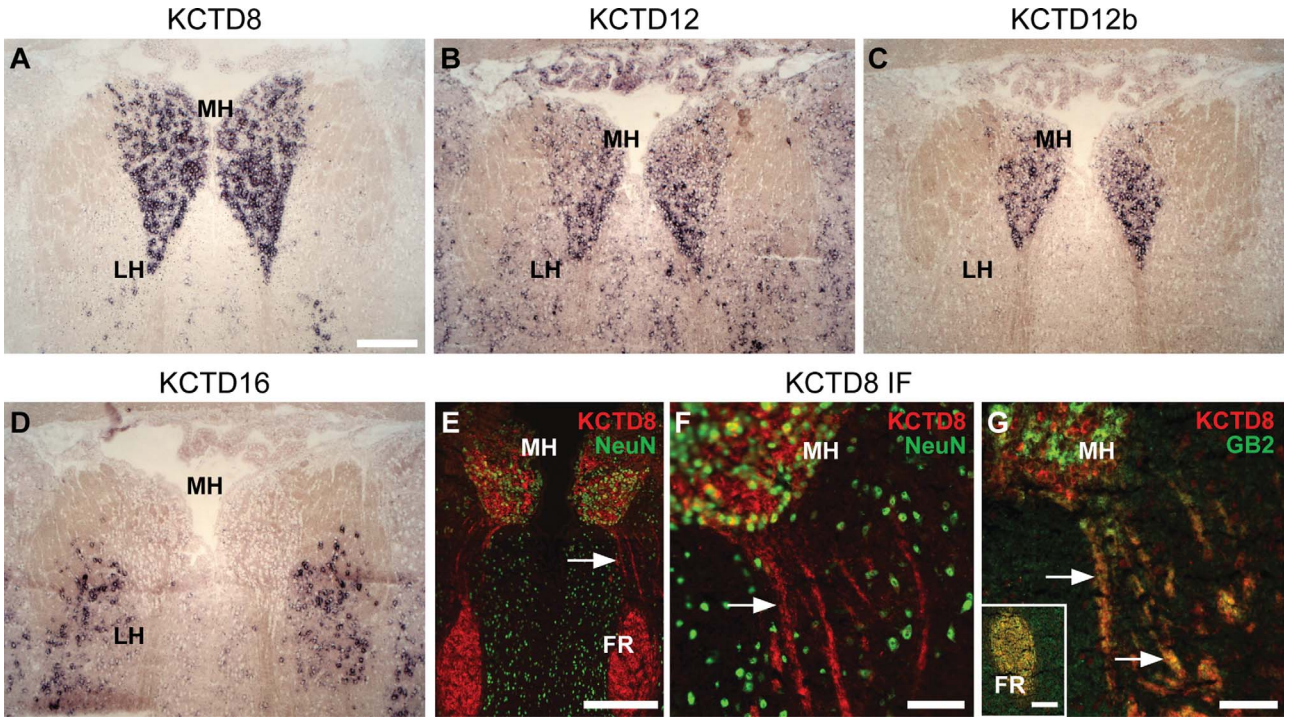

Figure 9. KCTD expression in the habenula of the adult mouse. KCTD8 (**A**), 12 (**B**), and 12b (**C**) are highly expressed in the medial habenula. KCTD16 transcripts (**D**) are only detectable in the lateral habenula. Immunofluorescence microscopy reveals high expression of KCTD8 protein (in red) in the neurons of the medial habenula and their axonal projections along the fasciculus retroflexus (arrow, **E,F**). Prominent colocalization of KCTD8 and $GABA_{B2}$ is observed in these axonal projections from the medial habenula (arrows, **G** and inset). IF, immunofluorescence; LH, lateral habenula; MH, medial habenula; FR, fasciculus retroflexus. A magenta-green copy of this figure is available as Supplementary Fig. 4. Scale bars = 200 μm in A–E; 100 μm in F,G.

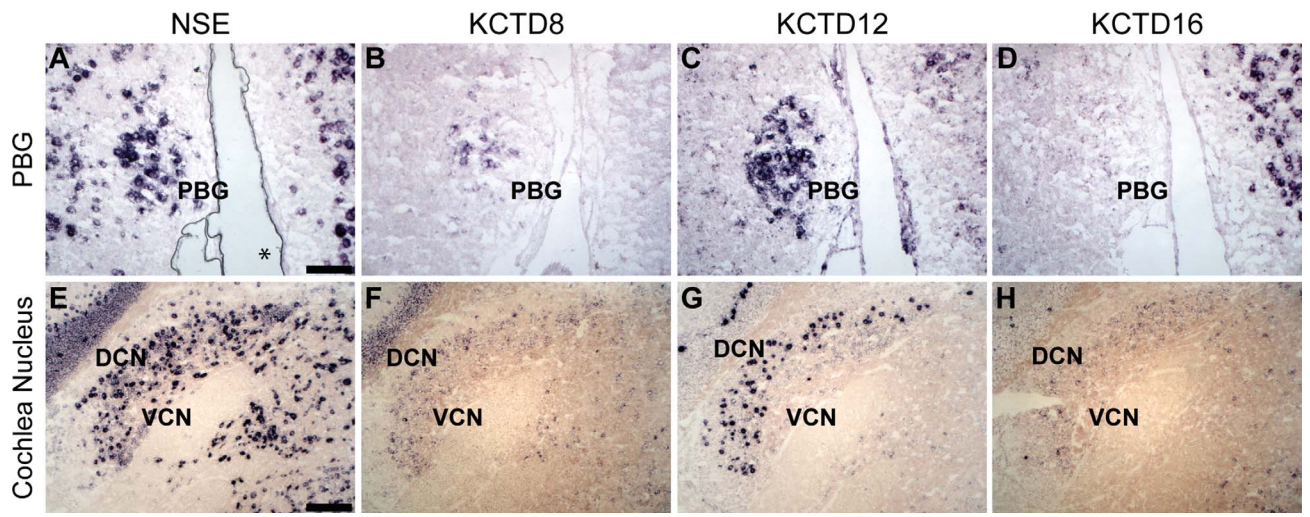

Figure 10. KCTD transcript distribution in the parabigeminal and the cochlear nucleus of the adult mouse. NSE expression is shown for comparison (**A,E**, asterisk in A indicates artifact of air inclusion). Neurons in the parabigeminal nucleus (PBG) express KCTD8 (**B**) and very high levels of KCTD12 mRNA (**C**). Similarly, KCTD8 and high levels of KCTD12 were found in the dorsal cochlea nucleus (DCN, **F,G**, respectively). KCTD16 is not detectable in the PBG (**D**) and shows very low expression levels in the cochlea nucleus (**H**). DCN, dorsal cochlea nucleus; PBG, parabigeminal nucleus; VCN, ventral cochlea nucleus. Scale bar = 100 μm for A–D; 200 μm for E–H.

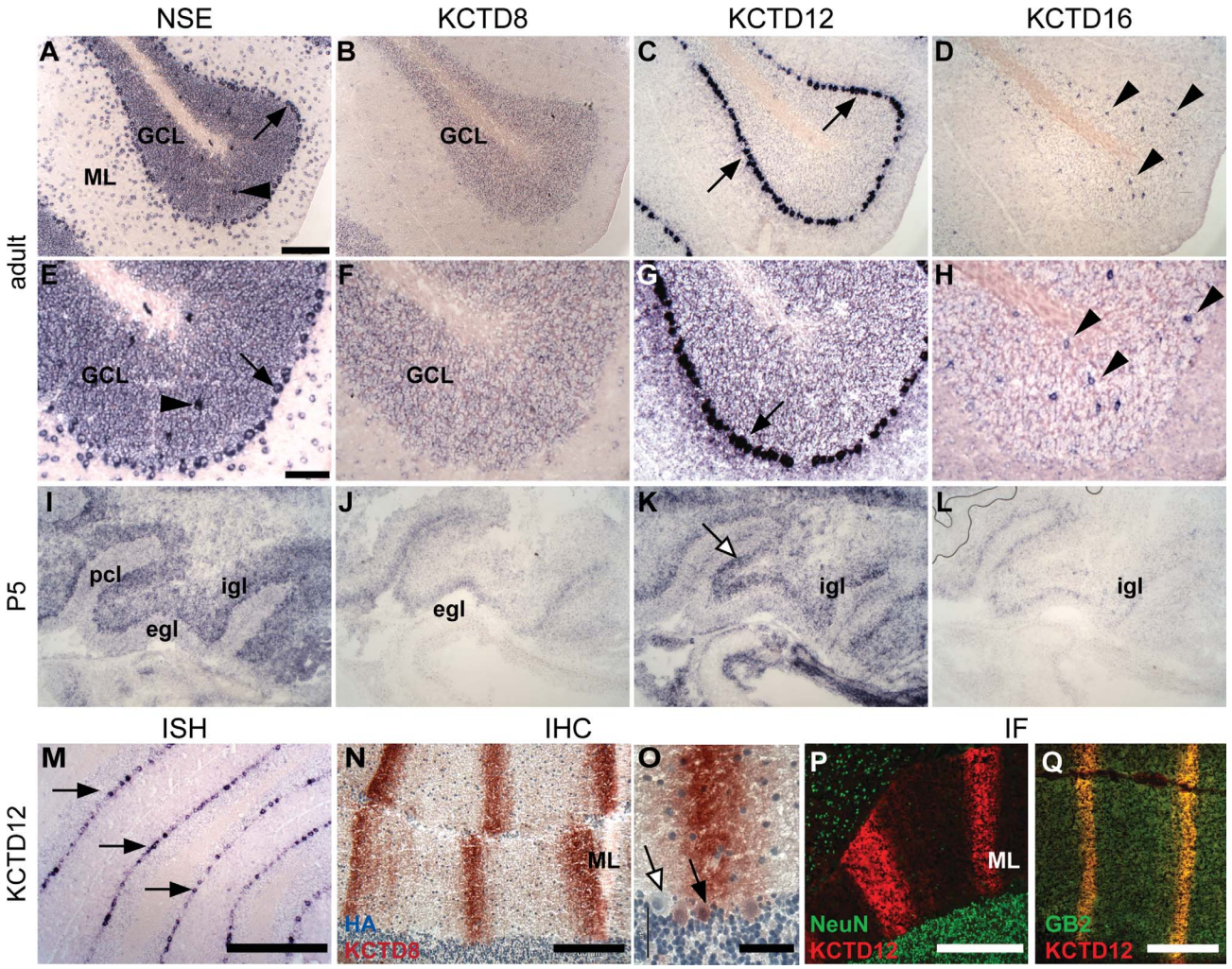

Figure 11. KCTD distribution in the mouse cerebellum. NSE expression is shown for comparison (**A,E,I**). Granule cells express KCTD8 (**B,F**), Purkinje cells KCTD12 (arrows, **C,G**), and putative Golgi cells KCTD16 transcripts (arrowheads, **D,H**). Hybridization of P5 brain sections reveals that KCTD8 transcripts are predominant in the external granular layer (egl, **J**) and KCTD12 transcripts in the internal granular layer and in migrating Purkinje cells (igl, open arrow, **K**). KCTD16 transcripts show very weak expression in the internal granular layer (igl, **L**). In the adult KCTD12 transcripts exhibit a zebrin-like expression pattern in Purkinje cells (arrows, **M**). Similarly, KCTD12 protein (in red) shows the zebrin-like expression in immunoperoxidase (**N,O**) and immunofluorescence (**P**) stainings. Note KCTD12 expressing (arrow) and nonexpressing (open arrow) Purkinje cells in panel O. The striped pattern of KCTD12 immunoreactivity in the molecular layer matches the pattern of $GABA_{B2}$ immunoreactivity (**Q**). egl, external granular layer; GCL, granule cell layer; igl; internal granular layer; ML, molecular layer; PCL, Purkinje cell layer of the cerebellum; HA, Haemalaun; IF, immunofluorescence; IHC, immunohistochemistry. A magenta-green copy of this figure is available as Supplementary Fig. 5. Scale bars = 200 μm in A–D,N,P; 100 μm in E–L; 1,000 μm in M; 50 μm in O,Q.

DISCUSSION

We recently reported that brain $GABA_B$ receptors, in addition to the core subunits $GABA_{B1a}$, $GABA_{B1b}$, and $GABA_{B2}$, incorporate the auxiliary subunits KCTD8, 12, 12b, and 16 (Schwenk et al., 2010). These KCTD proteins associate as tetramers with the C-terminus of the $GABA_{B2}$ subunit, which distinctly influences pharmacological and biophysical properties of the receptor response. KCTD12 was also found to be associated with $GABA_{B2}$ in an independent report (Bartoi et al., 2010). It is expected that KCTD proteins contribute to overt differences in $GABA_B$ responses between neurons and effectors (Cunningham and Enna, 1996; Bonanno et al., 1997; Cruz et al., 2004). Detailed information about KCTD expression patterns in the brain and in neuronal compartments is currently lacking. In order to rationalize the contribution of KCTD proteins to native $GABA_B$ responses we carried out a comprehensive analysis of KCTD8, 12, 12b, and 16 expression in the mouse brain.

KCTD transcript distribution

The core subunits $GABA_{B1a}$, $GABA_{B1b}$, and $GABA_{B2}$ are expressed throughout the brain, with the hippocampus,

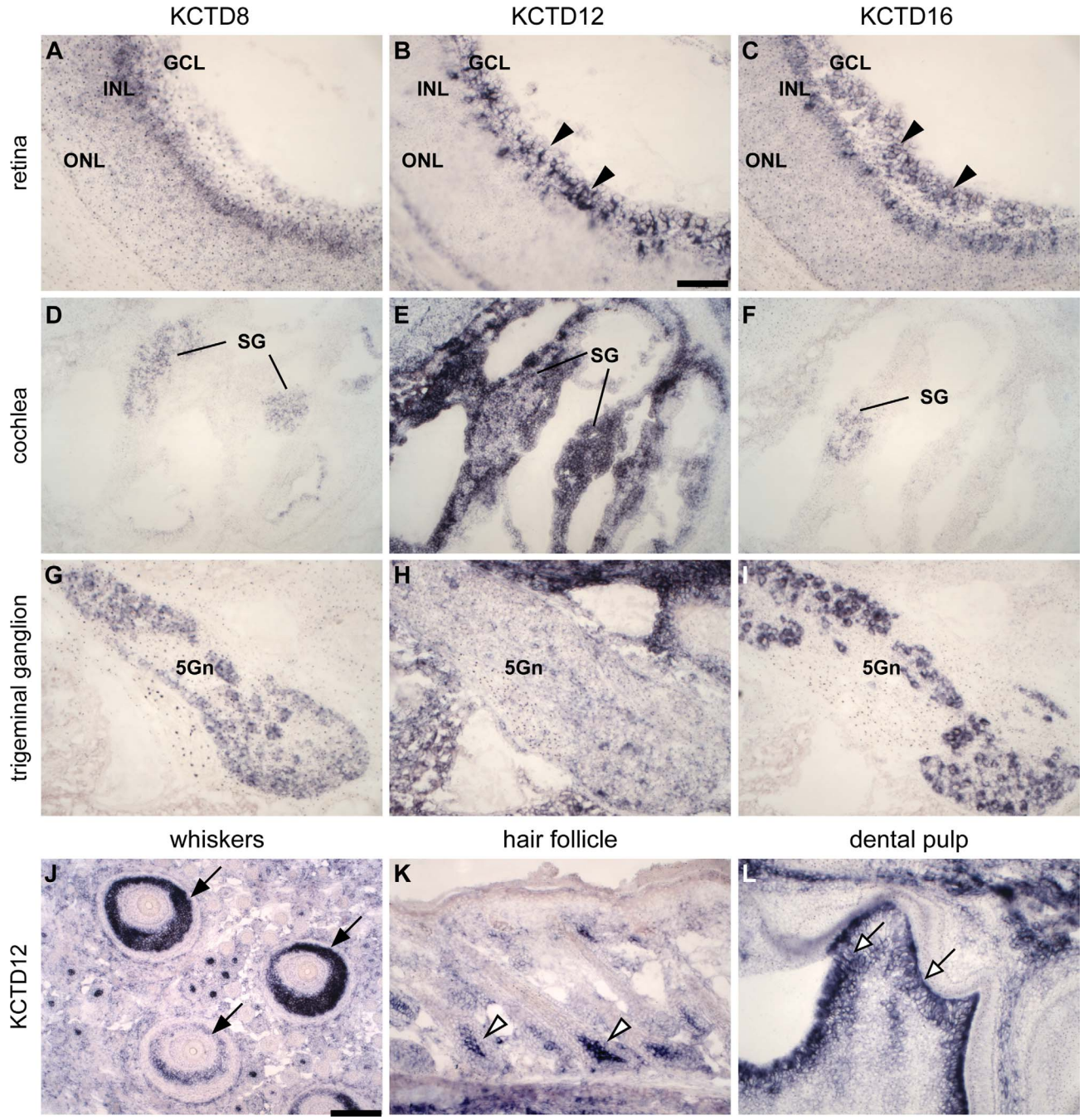

Figure 12. KCTD transcript distribution at P5 in sensory systems of the mouse. In the retina KCTD8 and 16 are expressed in the inner nuclear layer (**A,C**), KCTD12 and 16 in the ganglion cell layer (arrowheads, **B,C**). All KCTD transcripts are detectable in the spiral ganglia of the cochlea (**D–F**), with KCTD12 exhibiting very high expression levels (**E**). KCTD8 (**G**) and 16 (**I**) are highly, KCTD12 only marginally (**H**) expressed in the ganglion neurons of the trigeminus nerve. KCTD12 is strongly expressed in whisker follicles (arrows, **J**), hair follicles (open arrowheads, **K**), and in the odontoblast layer of the dental pulp (open arrows, **L**). GCL, ganglion cell layer; INL, inner nuclear layer; ONL, outer nuclear layer of the retina; SG, spiral ganglia of the cochlea; 5Gn, trigeminus nerve. Scale bars = 100 μm in A–I; 200 μm in J–L.

cerebellum, thalamus, and cerebral cortex demonstrating highest expression levels (Bischoff et al., 1999; Durkin et al., 1999; Fritschy et al., 2004). Likewise, we found that all major neuronal populations in the brain express transcripts for at least one KCTD subtype. This supports that all GABA$_B$ receptors in the brain incorporate KCTD proteins, in line with previous biochemical experiments (Schwenk et al., 2010). KCTDs have overlapping but distinct spatial and temporal distribution patterns, demonstrating that the repertoire of auxiliary GABA$_B$ subunits

varies among neuronal populations and during development. In general, KCTD12 and 16 transcripts are most ubiquitous and abundant. Pyramidal neurons and granule cells in the hippocampus coexpress transcripts for KCTD12 and 16, showing that KCTDs with very distinct influences on $GABA_B$ function (Schwenk et al., 2010) can reside in the same cells. Overall, KCTD16 transcripts exhibit a broad expression in the cortex, thalamus, and amygdala. KCTD12 transcripts are most abundant in specific nuclei or subsets of neurons. KCTD8 transcripts are enriched in a small subset of neurons, including neurons in the medial habenula, in several brain stem nuclei, and in cerebellar granule cells. KCTD12b is only present in the medial habenula. Some brain areas, such as the nuclei of the anterior dorsal thalamus, the globus pallidus, the claustrum, the medial septum, the hypothalamic preoptic area, or the mammillary bodies appear to express exclusively transcripts for one KCTD subtype (see Table 2). In contrast, several brain areas express transcripts for more than one KCTD, mostly in specific neuronal populations. In the cerebellum, for example, granule cells express KCTD8, Golgi cells KCTD16, and Purkinje cells KCTD12. Intriguingly, KCTD12 transcripts and protein in Purkinje cells exhibit the zebrin-like expression pattern that was already observed with $GABA_{B1}$ and $GABA_{B2}$ protein (Fritschy et al., 1999; Lujan and Shigemoto, 2006; Chung et al., 2008). In the cortex, pyramidal neurons in layer IV, VI, and the isocortex express KCTD16, whereas interneurons mostly express KCTD12. In summary, some $GABA_B$ receptor complexes in the brain appear to incorporate one particular KCTD subtype, while others potentially incorporate two or more distinct KCTD proteins. It is currently unknown whether distinct KCTD proteins can assemble into the same $GABA_B$ receptor complex and whether this imparts distinct properties to the receptor.

Subcellular distribution of KCTD proteins

Pyramidal neurons and dentate granule cells in the hippocampus express transcripts for both KCTD12 and 16. Previous ultrastructural analysis demonstrated that either of the proteins localizes to pre- and postsynaptic sites (Schwenk et al., 2010). Our immunohistochemical localization extends these findings and reveals that the two proteins are unequally distributed within granule cells. KCTD16 immunoreactivity is found in the soma and neuropil of dentate granule cells. In contrast, KCTD12 immunoreactivity is most prominent in the outer molecular layer, likely reflecting expression in distal dendrites. In this area dendritic spines of granule cells form synapses with entorhinal afferents of the perforant pathway (Nafstad, 1967). Strong KCTD12 immunoreactivity was also observed in the molecular layer of the cerebellum. Since specifically KCTD12 transcripts are expressed in Purkinje cells, KCTD12 protein must be mostly present on the dendritic arborization of Purkinje cells. This is in line with immunohistochemical studies demonstrating abundant postsynaptic $GABA_B$ receptors at parallel fiber-Purkinje cell synapses (Bischoff et al., 1999; Lujan and Shigemoto, 2006). The $GABA_{B1b}$ subunit mostly localizes to postsynaptic sites (Perez-Garci et al., 2006; Guetg et al., 2009) and is much more abundant than $GABA_{B1a}$ in Purkinje cells (Bischoff et al., 1999; Durkin et al., 1999; Margeta-Mitrovic et al., 1999). Dendritic $GABA_B$ receptors in Purkinje cells, therefore, mostly assemble from the $GABA_{B(1b,2)}$ core receptor and KCTD12 subunits. In contrast, axonal $GABA_B$ receptors in the fasciculus retroflexus projecting from the medial habenula to the interpeduncular nucleus (Bischoff et al., 1999; Fritschy et al., 2004) are presumably assembled with KCTD8. Thus, in some neurons KCTD8 and 12 proteins exhibit an axonal and dendritic polarization, respectively.

KCTD expression in glial cells and in peripheral tissues

Glial cells appear to marginally express KCTD proteins, which is consistent with generally low $GABA_B$ receptor expression levels in nonneuronal brain cells (Bischoff et al., 1999; Fritschy et al., 2004). Intriguingly, we found that KCTD12 transcripts and protein are highly abundant in olfactory ensheathing cells in the olfactory nerve layer. Olfactory ensheathing cells are the principal glial cells of the olfactory bulb and ensheath the axons of the olfactory nerve (Franklin and Barnett, 2000). Previous localization studies indicated that $GABA_B$ receptors are strongly expressed in olfactory receptor neurons but not in olfactory ensheathing cells (Bonino et al., 1999). It is therefore possible that KCTD12 in olfactory ensheathing cells assumes functions other than the modulation of $GABA_B$ receptors. Likewise, expression of KCTD8, 12, 12b, and 16 transcripts is observed in various mouse tissues not expected to express $GABA_B$ receptors. For example, Northern blot analysis detects KCTD12 expression in the intestine, kidney, heart, testis, adipose tissue, and bone marrow. KCTD12 protein was also reported to be a prognostic marker for gastrointestinal stromal tumors, showing an inverse relation to tumor metastasis (Suehara et al., 2008; Kikuta et al., 2010). Overall, this suggests that the role of KCTD12 extends beyond $GABA_B$ receptors.

ACKNOWLEDGMENT

The authors thank Beat Erne for technical advice and helpful discussions regarding immunohistochemistry and microscopy.

LITERATURE CITED

Bartoi T, Rigbolt KT, Du D, Kohr G, Blagoev B, Kornau HC. 2010. $GABA_B$ receptor constituents revealed by tandem affinity purification from transgenic mice. J Biol Chem 285: 20625–20633.

Bettler B, Kaupmann K, Mosbacher J, Gassmann M. 2004. Molecular structure and physiological functions of $GABA_B$ receptors. Physiol Rev 84:835–867.

Bischoff S, Leonhard S, Reymann N, Schuler V, Shigemoto R, Kaupmann K, Bettler B. 1999. Spatial distribution of $GABA_BR1$ receptor mRNA and binding sites in the rat brain. J Comp Neurol 412:1–16.

Bonanno G, Raiteri M. 1993. γ-Aminobutyric acid (GABA) autoreceptors in rat cerebral cortex and spinal cord represent pharmacologically distinct subtypes of the $GABA_B$ receptor. J Pharmacol Exp Ther 265:765–770.

Bonanno G, Fassio A, Schmid G, Severi P, Sala R, Raiteri M. 1997. Pharmacologically distinct $GABA_B$ receptors that mediate inhibition of GABA and glutamate release in human neocortex. Br J Pharmacol 120:60–64.

Bonino M, Cantino D, Sassoe-Pognetto M. 1999. Cellular and subcellular localization of γ-aminobutyric $acid_B$ receptors in the rat olfactory bulb. Neurosci Lett 274:195–198.

Brochu G, Maler L, Hawkes R. 1990. Zebrin II: a polypeptide antigen expressed selectively by Purkinje cells reveals compartments in rat and fish cerebellum. J Comp Neurol 291:538–552.

Chung SH, Kim CT, Hawkes R. 2008. Compartmentation of GABA B receptor2 expression in the mouse cerebellar cortex. Cerebellum 7:295–303.

Crick FC, Koch C. 2005. What is the function of the claustrum? Philos Trans R Soc Lond B Biol Sci 360:1271–1279.

Cruz HG, Ivanova T, Lunn ML, Stoffel M, Slesinger PA, Luscher C. 2004. Bi-directional effects of $GABA_B$ receptor agonists on the mesolimbic dopamine system. Nat Neurosci 7: 153–159.

Cunningham MD, Enna SJ. 1996. Evidence for pharmacologically distinct $GABA_B$ receptors associated with cAMP production in rat brain. Brain Res 720:220–224.

Deisz RA, Billard JM, Zieglgansberger W. 1997. Presynaptic and postsynaptic $GABA_B$ receptors of neocortical neurons of the rat in vitro: differences in pharmacology and ionic mechanisms. Synapse 25:62–72.

Durkin MM, Gunwaldsen CA, Borowsky B, Jones KA, Branchek TA. 1999. An in situ hybridization study of the distribution of the $GABA_{B2}$ protein mRNA in the rat CNS. Brain Res Mol Brain Res 71:185–200.

Franklin RJ, Barnett SC. 2000. Olfactory ensheathing cells and CNS regeneration: the sweet smell of success? Neuron 28: 15–18.

Franklin KBJ, Paxinos G. 2001. The mouse brain in stereotaxic coordinates, 2nd ed. San Diego, CA: Academic Press.

Fritschy JM, Meskenaite V, Weinmann O, Honer M, Benke D, Mohler H. 1999. $GABA_B$-receptor splice variants GB1a and GB1b in rat brain: developmental regulation, cellular distribution and extrasynaptic localization. Eur J Neurosci 11: 761–768.

Fritschy JM, Sidler C, Parpan F, Gassmann M, Kaupmann K, Bettler B, Benke D. 2004. Independent maturation of the $GABA_B$ receptor subunits $GABA_{B1}$ and $GABA_{B2}$ during postnatal development in rodent brain. J Comp Neurol 477: 235–252.

Gassmann M, Shaban H, Vigot R, Sansig G, Haller C, Barbieri S, Humeau Y, Schuler V, Muller M, Kinzel B, Klebs K, Schmutz M, Froestl W, Heid J, Kelly PH, Gentry C, Jaton AL, van der Putten H, Mombereau C, Lecourtier L, Mosbacher J, Cryan JF, Fritschy JM, Luthi A, Kaupmann K, Bettler B. 2004. Redistribution of $GABA_{B(1)}$ protein and atypical $GABA_B$ responses in $GABA_{B(2)}$-deficient mice. J Neurosci 24:6086–6097.

Guetg N, Seddik R, Vigot R, Turecek R, Gassmann M, Vogt KE, Brauner-Osborne H, Shigemoto R, Kretz O, Frotscher M, Kulik A, Bettler B. 2009. The $GABA_{B1a}$ isoform mediates heterosynaptic depression at hippocampal mossy fiber synapses. J Neurosci 29:1414–1423.

Kaupmann K, Schuler V, Mosbacher J, Bischoff S, Bittiger H, Heid J, Froestl W, Leonhard S, Pfaff T, Karschin A, Bettler B. 1998. Human γ-aminobutyric acid type B receptors are differentially expressed and regulate inwardly rectifying K^+ channels. Proc Natl Acad Sci U S A 95:14991–14996.

Kaupmann K, Cryan JF, Wellendorph P, Mombereau C, Sansig G, Klebs K, Schmutz M, Froestl W, van der Putten H, Mosbacher J, Brauner-Osborne H, Waldmeier P, Bettler B. 2003. Specific γ-hydroxybutyrate-binding sites but loss of pharmacological effects of γ-hydroxybutyrate in $GABA_{B(1)}$-deficient mice. Eur J Neurosci 18:2722–2730.

Kikuta K, Gotoh M, Kanda T, Tochigi N, Shimoda T, Hasegawa T, Katai H, Shimada Y, Suehara Y, Kawai A, Hirohashi S, Kondo T. 2010. Pfetin as a prognostic biomarker in gastrointestinal stromal tumor: novel monoclonal antibody and external validation study in multiple clinical facilities. Jpn J Clin Oncol 40:60–72.

Koulen P, Malitschek B, Kuhn R, Bettler B, Wässle H, Brandstätter JH. 1998. Presynaptic and postsynaptic localization of $GABA_B$ receptors in neurons of the rat retina. Eur J Neurosci 10:1446–1456.

Kulik A, Vida I, Lujan R, Haas CA, Lopez-Bendito G, Shigemoto R, Frotscher M. 2003. Subcellular localization of metabotropic $GABA_B$ receptor subunits $GABA_{B(1a/b)}$ and $GABA_{B(2)}$ in the rat hippocampus. J Neurosci 23:11026–11035.

Lai C, Lemke G. 1991. An extended family of protein-tyrosine kinase genes differentially expressed in the vertebrate nervous system. Neuron 6:691–704.

LeDoux JE. 2000. Emotion circuits in the brain. Annu Rev Neurosci 23:155–184.

LeDoux J. 2007. The amygdala. Curr Biol 17:R868–874.

Lee MT, Chen CH, Lee CS, Chen CC, Chong MY, Ouyang WC, Chiu NY, Chuo LJ, Chen CY, Tan HK, Lane HY, Chang TJ, Lin CH, Jou SH, Hou YM, Feng J, Lai TJ, Tung CL, Chen TJ, Chang CJ, Lung FW, Chen CK, Shiah IS, Liu CY, Teng PR, Chen KH, Shen LJ, Cheng CS, Chang TP, Li CF, Chou CH, Wang KH, Fann CS, Wu JY, Chen YT, Cheng AT. 2010. Genome-wide association study of bipolar I disorder in the Han Chinese population. Mol Psychiatry [Epub ahead of print].

Lin X, Chen S, Chen P. 2000. Activation of metabotropic $GABA_B$ receptors inhibited glutamate responses in spiral ganglion neurons of mice. Neuroreport 11:957–961.

Lopez-Bendito G, Shigemoto R, Kulik A, Paulsen O, Fairen A, Lujan R. 2002. Expression and distribution of metabotropic GABA receptor subtypes $GABA_BR1$ and $GABA_BR2$ during rat neocortical development. Eur J Neurosci 15: 1766–1778.

Lopez-Bendito G, Lujan R, Shigemoto R, Ganter P, Paulsen O, Molnar Z. 2003. Blockade of $GABA_B$ receptors alters the tangential migration of cortical neurons. Cereb Cortex 13: 932–942.

Lopez-Bendito G, Shigemoto R, Kulik A, Vida I, Fairen A, Lujan R. 2004. Distribution of metabotropic GABA receptor subunits $GABA_{B1a/b}$ and $GABA_{B2}$ in the rat hippocampus during prenatal and postnatal development. Hippocampus 14: 836–848.

Lujan R, Shigemoto R. 2006. Localization of metabotropic GABA receptor subunits $GABA_{B1}$ and $GABA_{B2}$ relative to synaptic sites in the rat developing cerebellum. Eur J Neurosci 23:1479–1490.

Maison SF, Casanova E, Holstein GR, Bettler B, Liberman MC. 2009. Loss of $GABA_B$ receptors in cochlear neurons: threshold elevation suggests modulation of outer hair cell function by type II afferent fibers. J Assoc Res Otolaryngol 10:50–63.

Malitschek B, Rüegg D, Heid J, Kaupmann K, Bittiger H, Fröstl W, Bettler B, Kuhn R. 1998. Developmental changes in agonist affinity at $GABA_{B(1)}$ receptor variants in rat brain. Mol Cell Neurosci 12:56–64.

Margeta-Mitrovic M, Mitrovic I, Riley RC, Jan LY, Basbaum AI. 1999. Immunohistochemical localization of $GABA_B$ receptors in the rat central nervous system. J Comp Neurol 405: 299–321.

Mullen RJ, Buck CR, Smith AM. 1992. NeuN, a neuronal specific nuclear protein in vertebrates. Development 116: 201–211.

Nafstad PH. 1967. An electron microscope study on the termination of the perforant path fibres in the hippocampus and the fascia dentata. Z Zellforsch Mikrosk Anat 76: 532–542.

Panzanelli P, Lopez-Bendito G, Lujan R, Sassoe-Pognetto M. 2004. Localization and developmental expression of $GABA_B$ receptors in the rat olfactory bulb. J Neurocytol 33:87–99.

Perez-Garci E, Gassmann M, Bettler B, Larkum ME. 2006. The $GABA_{B1b}$ isoform mediates long-lasting inhibition of dendritic Ca^{2+} spikes in layer 5 somatosensory pyramidal neurons. Neuron 50:603–616.

Pierau FK, Yakimova KS, Sann H, Schmid HA. 1997. Specific action of $GABA_B$ ligands on the temperature sensitivity of hypothalamic neurons. Ann N Y Acad Sci 813:146–155.

Princivalle A, Spreafico R, Bowery N, De Curtis M. 2000. Layer-specific immunocytochemical localization of $GABA_BR1a$ and $GABA_BR1b$ receptors in the rat piriform cortex. Eur J Neurosci 12:1516–1520.

Reis GM, Duarte ID. 2006. Baclofen, an agonist at peripheral $GABA_B$ receptors, induces antinociception via activation of TEA-sensitive potassium channels. Br J Pharmacol 149: 733–739.

Resendes BL, Kuo SF, Robertson NG, Giersch AB, Honrubia D, Ohara O, Adams JC, Morton CC. 2004. Isolation from cochlea of a novel human intronless gene with predominant fetal expression. J Assoc Res Otolaryngol 5:185–202.

Schaeren-Wiemers N, Gerfin-Moser A. 1993. A single protocol to detect transcripts of various types and expression levels in neural tissue and cultured cells: in situ hybridization using digoxigenin-labelled cRNA probes. Histochemistry 100:431–440.

Schaeren-Wiemers N, Andre E, Kapfhammer JP, Becker-Andre M. 1997. The expression pattern of the orphan nuclear receptor RORbeta in the developing and adult rat nervous system suggests a role in the processing of sensory information and in circadian rhythm. Eur J Neurosci 9: 2687–2701.

Schwenk J, Metz M, Zolles G, Turecek R, Fritzius T, Bildl W, Tarusawa E, Kulik A, Unger A, Ivankova K, Seddik R, Tiao JY, Rajalu M, Trojanova J, Rohde V, Gassmann M, Schulte U, Fakler B, Bettler B. 2010. Native $GABA_B$ receptors are heteromultimers with a family of auxiliary subunits. Nature 465:231–235.

Shaban H, Humeau Y, Herry C, Cassasus G, Shigemoto R, Ciocchi S, Barbieri S, van der Putten H, Kaupmann K, Bettler B, Luthi A. 2006. Generalization of amygdala LTP and conditioned fear in the absence of presynaptic inhibition. Nat Neurosci 9:1028–1035.

Sheerin AH, Nylen K, Zhang X, Saucier DM, Corcoran ME. 2004. Further evidence for a role of the anterior claustrum in epileptogenesis. Neuroscience 125:57–62.

Sloviter RS, Ali-Akbarian L, Elliott RC, Bowery BJ, Bowery NG. 1999. Localization of $GABA_B$ (R1) receptors in the rat hippocampus by immunocytochemistry and high resolution autoradiography, with specific reference to its localization in identified hippocampal interneuron subpopulations. Neuropharmacology 38:1707–1721.

Suehara Y, Kondo T, Seki K, Shibata T, Fujii K, Gotoh M, Hasegawa T, Shimada Y, Sasako M, Shimoda T, Kurosawa H, Beppu Y, Kawai A, Hirohashi S. 2008. Pfetin as a prognostic biomarker of gastrointestinal stromal tumors revealed by proteomics. Clin Cancer Res 14:1707–1717.

Sutherland RJ. 1982. The dorsal diencephalic conduction system: a review of the anatomy and functions of the habenular complex. Neurosci Biobehav Rev 6:1–13.

Swanson LW, Petrovich GD. 1998. What is the amygdala? Trends Neurosci 21:323–331.

Todd WM, Kafrawy AH, Newton CW, Brown CE Jr. 1997. Immunohistochemical study of gamma-aminobutyric acid and bombesin/gastrin releasing peptide in human dental pulp. J Endod 23:152–157.

Ulrich D, Bettler B. 2007. $GABA_B$ receptors: synaptic functions and mechanisms of diversity. Curr Opin Neurobiol 17: 298–303.

Vigot R, Barbieri S, Brauner-Osborne H, Turecek R, Shigemoto R, Zhang YP, Lujan R, Jacobson LH, Biermann B, Fritschy JM, Vacher CM, Muller M, Sansig G, Guetg N, Cryan JF, Kaupmann K, Gassmann M, Oertner TG, Bettler B. 2006. Differential compartmentalization and distinct functions of $GABA_B$ receptor variants. Neuron 50:589–601.

Zhang X, Hannesson DK, Saucier DM, Wallace AE, Howland J, Corcoran ME. 2001. Susceptibility to kindling and neuronal connections of the anterior claustrum. J Neurosci 21: 3674–3687.

Zilles K. 1990. Anatomy of the neocortex: cytoarchitecture and myeloarchitecture. In: Kolb B, Tees RC, editors. The cerebral cortex of the rat. Cambridge, MA: MIT Press. p 77–102.